

The Impact of Stocks on Correlations of Crop Yields and Prices and on Revenue Insurance Premiums using Semiparametric Quantile Regression

Matthew Stuart

Department of Mathematics and Statistics,
Center for Data Science and Consulting, Loyola University, Chicago
1032 W. Sheridan Road
Chicago, IL 60660
mstuart1@luc.edu

Cindy Yu

Department of Statistics, Iowa State University
2431 Osborn Drive
Ames, IA 50011
cindyyu@iastate.edu

David A. Hennessy

Department of Economics, Iowa State University
518 Farm House Ln.
Ames, IA 50011
hennessy@iastate.edu

Abstract:

Crop yields and harvest prices are often considered to be negatively correlated, thus acting as a natural risk management hedge through stabilizing revenues. Storage theory gives reason to believe that the correlation is an increasing function of stocks carried over from previous years. Stock-conditioned second moments have implications for price movements during shortages and for hedging needs, while spatially varying yield-price correlation structures have implications for who benefits from commodity support policies. In this paper, we propose to use semi-parametric quantile regression (SQR) with penalized B-splines to estimate a stock-conditioned joint distribution of yield and price. The proposed method, validated through a comprehensive simulation study, enables sampling from the true joint distribution using SQR. Then it is applied to approximate stock-conditioned correlation and

revenue insurance premium for both corn and soybeans in the United States. For both crops, Cornbelt core regions have more negative correlations than do peripheral regions. We find strong evidence that correlation becomes less negative as stocks increase. We also show that conditioning on stocks is important when calculating actuarially fair revenue insurance premiums. In particular, revenue insurance premiums in the Cornbelt core will be biased upward if the model for calculating premiums does not allow correlation to vary with stocks available. The stock-dependent correlation can be viewed as a form of tail dependence that, if unacknowledged, leads to mispricing of revenue insurance products.

1 Introduction

Storage infrastructure and the associated commodity stocks serve a critical role in ensuring resilience to commodity market shocks. Resilience in markets is reflected by the degree of price insensitivity to a shock, most typically a current-year yield response to underlying weather, disease or related production conditions. Price-yield correlation, being a normalized measure of how sensitive price is to a production shock, can measure both resilience and revenue stability for growers. Stocks carried into the current year can be drawn down to supplement consumption in an adverse yield event. How correlation changes with stocks can establish the value of stocks as a means to manage market shocks. As an empirical matter, little is known about how commodity stocks act to buffer price movements against a production shock. The intent of this paper is to accurately estimate the price-yield joint distribution when conditioned on stocks using semiparametric quantile regression methods, and then provide evidence on how stocks affect price variability, producer revenue variability, and revenue insurance premium calculation.

The matter is important for several reasons where perhaps the most important is in understanding the source of large and dramatic commodity price spikes. Price spikes often arise when stocks are low and are more frequent for commodities, such as electricity and fresh produce, that are difficult or impossible to store. For consumers, price variability reduces economic welfare under certain intuitive conditions (Turnovsky et al. (1980)), while for risk averse producers who cannot adapt decisions to variable prices, the impact is detrimental (Oi (1961), Bellemare et al. (2013)). A large, nuanced and as yet inconclusive literature has also investigated whether such price spikes act to cause political instability (Blair et al.

(2021), De Winne & Peersman (2021)).

A second motivation for inquiry into the issue regards our collective understanding of regional comparative advantage. Core-periphery theory emphasizes the advantages and disadvantages that a core region in a economic activity has relative to less central areas. Agglomeration economies, due to lower transportation, search, learning and other benefits associated with spatially concentrated economic activity, are often among the most prominent advantages possessed by the core (Puga (2010)). We follow others in documenting a natural hedge effect (Finger (2012)) whereby revenue is more stable in core crop production regions than in the periphery (Ramsey et al. (2019)). For example, low price and low yield are less likely to occur simultaneously in a core region than in a region more distant from the center of production. In consequence, production in the core region is comparatively less financially risky. In this light the availability of opportunities to insure against revenue shortfalls can be seen as a counterweight to this advantage. We go further in showing that the regional comparative advantage provided by the natural hedge is likely to be most important, in the event of a price spike caused by low current-year yield and low stocks carried into the year.

An additional stimulus for this study is more directly practical, having to do with modeling assumptions when pricing revenue insurance (RI), which was first offered in the mid-1990s and quickly became the most popular form of crop insurance offered in the United States.¹ As insurance is intended to indemnify in extreme events, modeling assumptions that apply on average but do not apply in tail events can prove to be problematic, (see Zimmer

¹RI indemnifies revenue shortfall relative to a reference revenue guarantee. An indemnification event can arise because of low yield or low price. Approximately 70% of policies sold are of this form.

(2012) among others). Biased probabilities of extreme outcomes may lead to biased premiums because payoffs are largest in extreme outcomes. Depending on the direction of any bias, the products may attract unduly high-risk business or may lead to low participation. If high crop insurance participation is a government policy goal, as is true in many parts of the world, then that government may be required to provide larger subsidies to secure the desired level of participation. Our interest in stocks (storage) arises because its presence potentially affects the joint price-yield distribution that determines crop insurance premium.

Accurately estimating the stock-conditioned joint price-yield distribution is crucial for calculating price-yield correlation and revenue insurance premiums. Relying solely on a purely parametric approach may lead to model misspecification, while a purely non-parametric approach may be heavily influenced by the dimensionality and sample size. To overcome these limitations, we propose a semiparametric quantile regression (SQR) approach that enables the sampling of valid draws from the target joint price-yield distribution, conditioned on stocks. These draws can then be utilized to estimate the moments of various functions involving price and yield through Monte Carlo averaging. Examples of such moments include the stock-conditional correlation between price and yield, as well as stock-conditional crop premium rates (i.e., the mean of indemnity payout which depends on price and yield).

Quantile regression estimates the τ -th quantile of the conditional density $g(x|\tilde{s})$, where \tilde{s} is stock and x could be a univariate variable like price, or a bivariate variable like (price, yield). By allowing τ to vary across the range $(0, 1)$, the entire spectrum of the conditional distribution is revealed. We define $q_\tau(\tilde{s})$ as the τ -th conditional quantile function, which is the inverse of the cumulative distribution function $G^{-1}(\tau|\tilde{s})$. Rather than estimating $g(x|\tilde{s})$ parametrically or non-parametrically, we use B-spline bases to estimate $q_\tau(\tilde{s})$ semiparametri-

cally. By the inverse probability transformation, we can obtain valid draws x_r^* ($r = 1, \dots, R$) from the target distribution $g(x|\tilde{s})$ via $x_r^* = \hat{q}_{\tau_r}(\tilde{s}) = \hat{G}^{-1}(\tau_r|\tilde{s})$, where τ_r is independently drawn from a uniform distribution over $(0, 1)$ and R could be a large number.

Our SQR-based random number generation method has several attractive features. First, it does not rely on strong model assumptions like a fully parametric approach, making it robust against model violations. Specifically, B-splines are used to estimate the τ -th quantile function for different τ values ranging from 0 to 1, allowing for flexibility in identifying potential non-linear relationships between x and \tilde{s} , as well as non-constant variance and non-constant skewness that are not easily captured by traditional Normal models. Second, the draws from the joint price-yield distribution can be easily generated by simulating random numbers from a Uniform(0,1) distribution, once the semiparametric estimates of the conditional quantile function $\hat{q}_\tau(\tilde{s})$ are obtained. This feature simplifies the sampling process and enhances its efficiency. Third, outliers can be easily avoided by controlling the simulated τ values to ensure that they are not too close to 0 or 1. We are not the first to use quantile regression in econometrics (Koenker (2000), Koenker & Hallock (2001)). More specifically, Liao & Wang (2012) used quantile regression techniques with spatial econometric modeling for hedonic pricing for housing valuation. Our paper is distinctive from those papers in terms of objective and estimation method: (1) We propose to simulate valid draws from a 2-dimensional joint density of crop yields and prices, while previous studies have focused only on estimating the univariate density of crop yields, and (2) we propose to estimate the quantile regression functions semiparametrically using penalized B-splines, while others have used a strictly non-parametric approach (Ramsey (2020), Goodwin & Ker (1998), Barnwal & Kotani (2013), Ker & Coble (2003))

The remainder of the paper is organized as follows. Section 2 discusses the conceptual framework of the theory of storage, and its implication on indemnities. Section 3 outlines in detail the procedures for SQR, the construction of the B-spline bases, and the sampling procedure from the joint distribution function. Section 4 demonstrates the validity of our methods using a thorough simulation study. Section 5 employs our method empirically on both corn and soybean datasets. Section 6 concludes with some final remarks.

2 Conceptual Framework

2.1 Theory of Storage

The theory behind the role of stocks in determining second moments of the price yield distribution can be summarized in two graphics. For a given acreage allocated to a crop but random yield from these acres, Figure 1 visualizes the traditional supply and demand relationship absent stocks. The horizontal axis reflects current-year production only. Demand is a stable function of commodity available with finite negative slope. To understand the supply side characterization, bear in mind that farm production is determined largely by either (i) acreage, seed and fertilizer input decisions made at or before planting or (ii) weather and disease conditions that are often entirely exogenous to production. For these reasons, the short-run supply function is held to be vertical, or unresponsive to price, and stochastic where this randomness is characterized by good-year and bad-year yield outcomes either side of the vertical average year supply curve. Visible in Figure 1 is what might be termed “the farmer’s curse” whereby a good harvest, presuming that it is good for all producers, leads to

low prices so that revenue might decline in good years. If the demand curve is very inelastic, and so the correlation between a production shock and price is strongly negative, then a positive yield shock will decrease revenue. In fact this phenomenon is an extreme outcome of one of two manifestations of the natural hedge where the farmer must also recognize the associated event that prices rise when supplies are limited.

Including storage fundamentally changes the price quantity relationship (Stüttgen et al. (2018)). With storage then good-year product that would obtain a low price were it sold in that year can be stored in the hope that an average or bad year will follow so that prices will rise. Then the stored product purchased at a low price can be sold at a price high enough to compensate for storage costs. The activity is inherently risky, however, because storage costs are certain but future harvests are random. A storer will incur a loss in the event of several good-year harvests. Figure 2 visualizes how Deaton & Laroque (1992) characterizes the availability of stored stocks for consumption and how it should relate to current market price were decision makers acting rationally. When compared with Figure 1, storage is allowed in Figure 2 so that the horizontal axis includes both (i) current-year quantity and (ii) stocks carried over from prior years. The downward sloping price-to-stocks curve of Figure 2 is a demand curve, but does not necessarily represent demand for current year consumption. Professional storers are assumed to be risk neutral in Deaton & Laroque (1992) and the key decision is whether product (either from last year or newly harvested) is to be (a) placed on the market for consumption or (b) stored instead. Product will be stored whenever expected future price is sufficiently high relative to the current price. Otherwise product will be sold for current consumption. Market forces, i.e., arbitrage activities, will generally ensure that the allocation between storage and current consumption is such that

prices align and commodity owners are indifferent between the sell or store choice.

However, a corner solution may arise in the event of a sequence of poor harvests or alternatively when one very poor harvest occurs and little stored commodity is available, and the demand for the product right now may be such that no commodity is placed in storage, a situation that is called a stock-out. Deaton & Laroque (1992) use the i.i.d. random harvest assumption together with operator theory to establish that the relationship between available stocks (from storage or current harvest) and price is as given by the solid, continuous, two-part curve in Figure 2. The vertical red arrow shows how storage acts to buttress price when supplies are large. Rather than take a low price on the saturated market for current consumption, stocks are stored in the expectation that prices will rise in a year or two. When a stock-out occurs, then price is determined entirely by the current demand curve. However, when stocks exceed a critical level and price is lower than a corresponding critical price then additional stocks available due to a larger harvest are split into two uses. One is additional current consumption and the other is additional storage.

One interpretation of Figure 2 is to view the horizontal axis as consumption but then recognize that what you see is not what you get because when prices are low then not all additional harvest translates into additional stocks and the price decline is ameliorated. In shifting up the price to stocks curve when stocks are high, the presence of storage should reduce the adverse effect of higher harvest yield on price. Intuitively, this implies that

$$\text{Cor}(y_{jt}, p_t | \tilde{s}_t, l) \leq 0, \text{ and} \tag{1a}$$

$$\frac{d\text{Cor}(y_{jt}, p_t | \tilde{s}_t, l)}{d\tilde{s}_t} \geq 0, \tag{1b}$$

where y_{jt} is the harvested crop yield for county j in year t , p_t is the year t harvest price, s_t

is the actual amount of carryover stocks in from year $t - 1$ to year t , $\tilde{s}_t = \frac{s_t}{\tilde{x}_{t-1}}$ – the amount of production-normalized carryover stocks from year $t - 1$ to year t^2 , and \tilde{x}_{t-1} is a localized estimated scatterplot smoothing (LOESS) regression estimate of year $t - 1$'s national yield. We also view the correlation as being influenced by distance from the core production region as measured by l . Yields in any year are positively spatially correlated (Goodwin (2001), Gong et al. (2023)) because soils and weather events are positively spatially correlated. Therefore any core or central production region will have a large impact in determining price and price-yield correlations should be most strongly negative in core production regions. This natural hedge in turn generates a comparative advantage in risk management to these regions because low prices and low yield are unlikely to occur simultaneously. In our empirical data study, we will outline this natural hedge by showing that states in the core production region have large negative price-yield correlations for low stocks and less negative correlation for higher stocks, while states outside the core production region have price-yield correlation that is consistent for all possible levels of stocks.

Also of relevance to us from Deaton & Laroque (1992) is

$$\frac{d\text{Var}(p_t|\tilde{s}_t)}{d\tilde{s}_t} \leq 0. \quad (2)$$

Variability of price to stocks will decline with an increase in stocks because when stocks are low then additional current-year yield is consumed and so is devoted entirely to reducing current scarcity. When stocks are high then some of the addition is stored and not marketed,

²We normalize by production because when typical production and consumption is larger then more stocks is be needed to protect against the costs of future production shortfalls. Corn and soybean production has expanded over time as the human population has increased, demand for meat has expanded and more corn has been diverted to produce biofuels

lessening the impact on current price. This point is relevant for commodity markets because one price variability metric is implied volatility, as often extracted from applying the Black formula for options market prices on commodity futures (Black (1976)). It is well-known that stocks carried over from prior years decrease futures price volatility (Hennessy & Wahl (1996), Karali & Power (2013)). Our empirical data analysis will provide further evidence that as stocks increase, the volatility of the futures price decreases.

2.2 Setting Premium Rates and Implication for Indemnities

Private sector crop insurance offerings have been around for many years in the United States (Gardner (2002)), but have generally not been popular due to high administration costs and more recently due to competition from federal programs. Motivated by concerns about market failures (Chambers (1989); Just et al. (1999)), political considerations (Innes (2003)) and behavioral attitudes that depress demand (Du et al. (2017), Cai et al. (2020)), government support for agricultural insurance is often large. These supports take the forms of paying for infrastructure required to assess risks and of providing subsidies on premiums charged by insurance agents. Experiences in many countries and for many crops have shown that both intervention types are central to developing the levels of sustained grower participation in crop insurance that policy-makers seek (Kramer et al. (2022)). The product development path traversed by first the United States and more recently, India, China, European Union countries and elsewhere is not unexpected. Take-up is initially limited so contract design and pricing issues are repeatedly revisited, sometimes drawing in more growers and sometimes not (Ming et al. (2016), Santeramo & Ramsey (2017), Smith & Glauber (2019), Cariappa

et al. (2021)).

While impressive strides have been made in improving rate-setting in the United States (Coble et al. (2010)), problems remain (Ramirez & Carpio (2012); Price et al. (2019) Schnitkey et al. (2022)). A common complaint, which we refer to as spatial adverse selection, is that rate structures are such that farmers operating better quality land within a county are being asked to cross-subsidize those owning worse quality land under the same crop in that county (Ramirez & Shonkwiler (2017), Price et al. (2019)). Other sources of variabilities, such as year-to-year weather effects, (Ten & Zhang (2023)) in crop insurance value for farmers can also be problematic, as they may be visible and yet not factored into rate-setting processes. The subject of our investigation is accumulated stocks carried from year $t - 1$ to year t , where most of the main crops in plant agriculture can be stored across the typical harvest period at an acceptable cost.

The presence of stocks affects the joint distribution of price-yield, thus impacting the insurance premium setting. In functional form, the indemnity I_{jt} for a county j in year t is $I_{jt} = \max(\psi \bar{p}_t \bar{y}_t - p_t y_{jt}, 0)$, a decreasing and convex function of revenue ($p_t y_{jt}$) where \bar{p}_t is the year t spring futures price, \bar{y}_t is the actual production history (APH) yield average for year t , the arithmetic average of the past ten years of yield data, as required by federal regulation when available (Coble et al. (2010)), and ψ is the coverage rate of the insurance policy. The premium or expected indemnity payout for county j in year t can be calculated as

$$Premium_{jt} = E[I_{jt}] = \int \max(\psi \bar{p}_t \bar{y}_t - p_t y_{jt}, 0) dG(y_{jt}, p_t) \quad (3)$$

where $G(y_{jt}, p_t)$ is the cumulative distribution function for y_{jt} and p_t with associated density

function $g(y_{jt}, p_t)$.

In our empirical inquiry, we argue that $\text{Var}(p_t)$ and $\text{Cor}(y_{jt}, p_t) = \frac{\text{Cov}(y_{jt}, p_t)}{\sqrt{\text{Var}(y_{jt})\text{Var}(p_t)}}$ depend on \tilde{s}_t and location, and should be calculated with respect to a location-specific conditional density, $g(y_{jt}, p_t | \tilde{s}_t, c_j)$, where c_j is the state in which county j is located. In particular, we seek to characterize how the conditional correlation changes with stocks and location (i.e. state) and how conditional variance changes with stocks. Furthermore, if these effects are not fully accounted for in the insurance premium determination formula, then potential heterogeneity issues may impede insurance program participation and/or require additional subsidies to overcome. In addition, as the correlation is likely to be most negative in years with high price and low production, the stabilization effect of the natural hedge may not be adequately acknowledged by any insurance pricing formula. This inference supports the view that core production regions may face premiums that are too high in comparison to long run indemnities incurred, a view that is supported by empirical study of insurance program performance (Chen et al. (2020)). Current RI rate setting procedures for the corn and soybean crops in the United States identify mean prices through pre-planting futures prices for harvest-time contracts and identify price variability through implied volatilities extracted from relevant options prices. These estimates should be dynamic to stocks and other forms of information. However, no relevant financial instrument is available for correlation and no effort is made to condition correlation on market information. Thus, the bias of traditional premium calculation methods will be real to the extent that (1a), (1b), and (2) apply.

3 Methodology

Define $g(p_t|\tilde{s}_t)$ and $g(y_{jt}|p_t, \tilde{s}_t, c_j)$ as the density functions of p_t conditioning on \tilde{s}_t and of y_{jt} conditioning on p_t , \tilde{s}_t , and c_j , respectively, where it follows that $g(y_{jt}, p_t|\tilde{s}_t, c_j) = g(p_t|\tilde{s}_t)g(y_{jt}|p_t, \tilde{s}_t, c_j)$. Because p_t is a national harvest price, $g(p_t|\tilde{s}_t)$ does not depend on state c_j . For the sake of simplicity, we exclude c_j from the condition and fit the model separately for different states. For $\tau_p \in (0, 1)$ and $\tau_y \in (0, 1)$, let $q_{\tau_p}(\tilde{s})$ and $q_{\tau_y}(p, \tilde{s})$ denote the τ_p^{th} - and τ_y^{th} - conditional quantile functions of $g(p|\tilde{s})$ and $g(y|p, \tilde{s})$, respectively. By definition they are equal to the inverse cumulative distribution functions (cdfs) $G^{-1}(\tau_p|\tilde{s})$ and $G^{-1}(\tau_y|p, \tilde{s})$, i.e.,

$$q_{\tau_p}(\tilde{s}) = G^{-1}(\tau_p|\tilde{s}), \text{ and} \tag{4}$$

$$q_{\tau_y}(p, \tilde{s}) = G^{-1}(\tau_y|p, \tilde{s}). \tag{5}$$

Using semi-parametric quantile regression, we can estimate the possibly non-linear quantile functions $q_{\tau_p}(\tilde{s})$ and $q_{\tau_y}(p, \tilde{s})$ as $\hat{q}_{\tau_p}(\tilde{s})$ and $\hat{q}_{\tau_y}(p, \tilde{s})$, respectively. Therefore, by the inverse probability transformation, if $\tau_{p,r}$ and $\tau_{y,r}$ ($r = 1, 2, \dots, R$) are independently drawn from the uniform distribution on $(0, 1)$, then $p_r^* = \hat{q}_{\tau_{p,r}}(\tilde{s})$ and $y_r^* = \hat{q}_{\tau_{y,r}}(p_r^*, \tilde{s})$ provide independent random samples from the conditional joint density $g(y, p|\tilde{s})$.

Multiple choices exist for estimating $q_{\tau_p}(\tilde{s})$ and $q_{\tau_y}(p, \tilde{s})$, such as kernel weighting methods (Yu & Jones (1998)) and smoothing spline methods (Koenker et al. (1994)). Among all the literature findings, one important conclusion is that there exists a significant tradeoff between computational efficiency and smoothness of the regression estimates. Specifically, unsmoothed quantile regression methods are computationally efficient, but can produce spiky distributional curves, whereas smoothed regression methods produce a smoother distribu-

tional curve, but come at increased computational cost for calculating the “best” smoothing value. For this paper, we employ a quantile regression method based on penalized B-splines (Yoshida (2022), Chen & Yu (2016)). This approach provides a relatively smoothed quantile function that comes at reduced computational burden, without specifying a form of the quantile function. Figure 3 presents quantile function curves at different τ values; the uneven spacing between the curves suggests potential skewness or/and heavy tails in the target conditional distribution.

In Section 3.1, we introduce the generic ideas of quantile functions, quantile regression, and SQR with penalized B-splines. In Section 3.2, we outline our methodology to sample from $g(y_{jt}, p_t | \tilde{s}_t)$ using SQR with penalized B-splines.

3.1 SQR with Penalized B-Splines

Define y_i , $i = 1, \dots, n$ as observations from a generic response variable $Y \in \mathbb{R}$ and $\mathbf{x}_i = \{x_{1i}, x_{2i}, \dots, x_{di}\}^T$, $i = 1, \dots, n$ as a $d \times 1$ vector of observed covariates $\mathbf{X} \in (\chi_1 \times \dots \times \chi_d)$ where $\chi_l \subset \mathbb{R}$ for $l = 1, \dots, d$ is the compact space in which X_l is exclusively contained. In the specific context of our study, we can set $y_i = p_t$ and $\mathbf{x}_i = \tilde{s}_t$ for estimating $g(p_t | \tilde{s}_t)$, and set $y_i = y_{jt}$ and $\mathbf{x}_i = \{p_t, \tilde{s}_t\}^T$ for estimating $g(y_{jt} | p_t, \tilde{s}_t)$.

For $\tau \in (0, 1)$, the conditional quantile function $q_\tau(\mathbf{x})$ is defined as a function that satisfies $\text{Prob}(y \leq q_\tau(\mathbf{x}) | \mathbf{x}) = \tau$. One way to understand quantile regression is through replacing the squared error loss function in traditional linear least squares regression with the absolute deviation loss function, or check loss function,

$$\rho_\tau(y - q_\tau(\mathbf{x})) = (y - q_\tau(\mathbf{x})) \times (\tau - I\{y - q_\tau(\mathbf{x}) < 0\}), \quad (6)$$

as first defined in Koenker & Bassett (1978), where I represents the indicator function. Note that (6) is τ -specific; that is, each unique $\tau \in (0, 1)$ introduces a different loss function. Figure 4 visualizes the differences in the check loss function for eight equally spaced values of τ from 0.01 to 0.99. Intuitively, when we are interested in the 1st-quantile (i.e., $\tau = 0.01$), the slope of the check loss function (solid red curve in Figure 4) is much steeper in the negative direction than in the positive, meaning that the smaller observations contain more information about this small quantile than do the larger observations. As τ increases, the slope in the negative direction decreases and the slope in the positive direction increases; meaning that more weight is being placed on the larger observations than on the smaller ones for larger quantiles (e.g. dashed purple line for $\tau = 0.85$).

To address the issue of potential non-linearity in $q_\tau(\mathbf{x})$, we propose an SQR method using penalized B-splines. That is, we define the τ^{th} -quantile function as $q_\tau(\mathbf{x}) = \mathbf{B}^T(\mathbf{x})\boldsymbol{\beta}_\tau$ where $\mathbf{B}(\mathbf{x}) = \{\mathbf{B}_1^T(x_1), \dots, \mathbf{B}_d^T(x_d)\}^T$, $\{\mathbf{B}_l : \chi_l \rightarrow \mathbb{C}^{p+K_n}\}$ for $l = 1, \dots, d$ is the B-spline basis function that converts a scalar $x \in \chi_l$ to a value in $\mathbb{C}^{p+K_n} = \{\mathbf{z} \in \mathbb{R}^{p+K_n} : \sum_{m=1}^{p+K_n} z_m = 1, z_m \geq 0, m = 1, \dots, p + K_n\}$, p and $K_n - 1$ are the degree and number of knots of the B-spline basis, respectively. And $\boldsymbol{\beta}_\tau$ is the τ^{th} -quantile regression coefficients with $(p + K_n) \times 1$ dimension. B-splines offers a relatively smooth quantile regression function without requiring a specific functional form for the regression mean. Furthermore, the quantile function at specific τ values can take on diverse non-linear forms, enabling B-splines to effectively capture skewness and heteroskedasticity in the conditional distribution. This flexibility empowers us to refrain from imposing rigid assumptions regarding the shape of the distribution.

Details about the construction of the B-spline bases can be found in Section A of the online supplement, and readers can learn more properties that splines possess in (de Boor

(1978)). The estimated quantile regression function is then defined as

$$\hat{q}_\tau(\mathbf{x}) = \mathbf{B}^T(x)\hat{\boldsymbol{\beta}}_\tau, \text{ where}$$

$$\hat{\boldsymbol{\beta}}_\tau = \min_{\boldsymbol{\beta}} \sum_{i=1}^n \rho_\tau(y_i - \mathbf{B}^T(\mathbf{x}_i)\boldsymbol{\beta}) + \frac{\lambda}{2}\boldsymbol{\beta}^T \mathbf{D}_m^T \mathbf{D}_m \boldsymbol{\beta}. \quad (7)$$

Here $\lambda(> 0)$ is the quantile regression smoothing parameter, and \mathbf{D}_m is the m^{th} difference matrix defined as a $(K_n + p - m) \times (K_n + p)$ matrix with elements

$$d_{ij} = \begin{cases} (-1)^{|i-j|} \binom{m}{|i-j|} & 0 \leq |i-j| \leq m \\ 0 & \text{otherwise,} \end{cases}$$

where $\binom{m}{|i-j|} = \frac{m!}{|i-j|!(m-|i-j|)!}$. The penalty term in (7) is used to remove computational difficulties occurring when this term is defined through an integral, and controls the smoothness of the estimator (Yoshida (2022)). As λ increases, the estimated function becomes smoother. When $m = 2$, \mathbf{D}_m has an interpretation related to the integral of the square of the second derivative of the function defined by the B-spline. \mathbf{D}_2 is the choice of penalty matrix we use for the rest of this discussion, and the λ , K_n , and p choices will be discussed in the simulation study. The method is implemented to estimate two quantile functions $\hat{q}_{\tau_p}(\tilde{s})$ and $\hat{q}_{\tau_y}(p, \tilde{s})$ in equations (4) and (5), which are used to generate draws from $g(y, p|\tilde{s})$.

3.2 Sampling from the conditional distribution $g(y, p|\tilde{s})$

To correctly examine the impact of stocks on correlation and insurance premiums by utilizing aggregated data from multiple years, we must address two issues. Firstly, there may exist temporal correlations between the county-level yields and national harvest price of the current year and the observations from previous years. Secondly, the harvest price has not

been adjusted for inflation, which can potentially lead to misleading conclusions regarding the influence of stocks. To address the first issue, we mitigate it by detrending each of these variables. This involves converting y_{jt} and p_t to detrended variables, denoted as \tilde{y}_{jt} and \tilde{p}_t , respectively. We then apply our method on these detrended variables to obtain samples $\{\tilde{y}_r^*, \tilde{p}_r^*\}_{r=1}^R$ from the distribution of detrended yield and price, represented as $g(\tilde{y}, \tilde{p}|\tilde{s})$. Subsequently, we perform retrending to obtain samples $\{y_r^*, p_r^*\}_{r=1}^R$ from the distribution $g(y, p|\tilde{s})$. To tackle the second issue, we address it by adjusting the samples $\{y_r^*, p_r^*\}_{r=1}^R$ using the GDP deflator for prices and the estimated yield trends for yields. This adjustment allows us to obtain the adjusted samples $\{y_{a,r}^*, p_{a,r}^*\}_{r=1}^R$, where the yields and prices are expressed in units corresponding to year a . Section B in the online supplement discusses the method used to convert the price p_t and county-level yield y_{jt} to units corresponding to year a . In this paper, we have chosen to set $a = 2020$. Now, we will provide a description of our sampling procedure.

For p_t , we set \tilde{p}_t to be the difference between year t 's log-harvest price and a regression estimate of the log harvest price. More specifically, we set

$$\tilde{p}_t = \log(p_t) - \hat{p}_t, \tag{8}$$

where \hat{p}_t is a regression estimate of $\log(p_t)$ using localized estimated scatterplot smoothing (LOESS) regressed on year t . We do not detrend using the spring future's price because those detrended prices do not capture the trend as well as other smoothing methods.

For y_{jt} , we perform a penalized B-spline regression for mean yearly crop yield by state. Define a B-spline basis for this regression with $p = 3$, $K_n = \lceil \frac{T}{10} \rceil$, $\chi_t = [0, T]$, and evenly

knots spaced every 10 years. We estimate the year t trend \hat{y}_t to be

$$\hat{y}_t = \mathbf{B}^T(t)\hat{\boldsymbol{\beta}}, \quad (9)$$

$$\hat{\boldsymbol{\beta}} = \min_{\boldsymbol{\beta}} \sum_{t=1}^T \sum_{j=1}^{n_t} (y_{jt} - \mathbf{B}^T(t)\boldsymbol{\beta})^2 + \frac{\lambda}{2} \boldsymbol{\beta}^T \mathbf{D}_2^T \mathbf{D}_2 \boldsymbol{\beta}, \quad (10)$$

where n_t is the number of county-level data points in the given state, and the detrended county-level yield, \tilde{y}_{jt} , to be

$$\tilde{y}_{jt} = y_{jt} - \hat{y}_t. \quad (11)$$

Using SQR with penalized B-splines, we obtain the estimated quantile functions for detrended prices and yields as

$$\hat{q}_{\tau_p}(\tilde{s}) = \mathbf{B}^T(\tilde{s})\hat{\boldsymbol{\beta}}_{\tau_p} \text{ and} \quad (12)$$

$$\hat{q}_{\tau_y}(\tilde{p}, \tilde{s}) = \mathbf{B}^T(\tilde{p}_t, \tilde{s}_t)\hat{\boldsymbol{\beta}}_{\tau_y}, \quad (13)$$

where $\mathbf{B}(\tilde{p}, \tilde{s}) = \{\mathbf{B}^T(\tilde{p}), \mathbf{B}^T(\tilde{s})\}^T$; $\mathbf{B}(\tilde{p}_t)$ and $\mathbf{B}(\tilde{s}_t)$ are constructed using a method to be outlined in Section A of the online supplement and the choice p and K_n are discussed in the simulation study;

$$\hat{\boldsymbol{\beta}}_{\tau_p} = \min_{\boldsymbol{\beta}} \sum_{t=1}^T \rho_{\tau_p}(\tilde{p}_t - \mathbf{B}^T(\tilde{s}_t)\boldsymbol{\beta}) + \frac{\lambda}{2} \boldsymbol{\beta}^T \mathbf{D}_2^T \mathbf{D}_2 \boldsymbol{\beta}; \text{ and} \quad (14)$$

$$\hat{\boldsymbol{\beta}}_{\tau_y} = \min_{\boldsymbol{\beta}} \sum_{t=1}^T \sum_{j=1}^{n_t} \rho_{\tau_y}(\tilde{y}_{jt} - \mathbf{B}^T(\tilde{p}_t, \tilde{s}_t)\boldsymbol{\beta}) + \frac{\lambda}{2} \boldsymbol{\beta}^T \mathbf{D}_2^T \mathbf{D}_2 \boldsymbol{\beta}. \quad (15)$$

For the calculation of (10), (14) and (15), the value of the smoothing parameter, λ , is chosen via a generalized approximate cross-validation technique (Yuan (2006)).

For a given year with $\tilde{s}_t = \tilde{s}$, R independent samples from the joint distribution of detrended yields and prices are obtained as $\{\tilde{p}_r^* = \hat{q}_{\tau_p, r}(\tilde{s}), \tilde{y}_r^* = \hat{q}_{\tau_y, r}(\tilde{p}_r^*, \tilde{s})\}_{r=1}^R$, where $\{\tau_{p, r}\}_{r=1}^R$

and $\{\tau_{y,r}\}_{r=1}^R$ are randomly sampled from $Uniform(0, 1)$. Based on (8) and (11), we can perform retrending as $p_r^* = \exp(\hat{p}_t + \tilde{p}_r^*)$ and $y_r^* = \hat{y}_t + \tilde{y}_r^*$. Then $\{p_r^*, y_r^*\}_{r=1}^R$ are further converted into the year 2020 units, i.e. $\{p_{2020,r}^*, y_{2020,r}^*\}_{r=1}^R$, according to the adjustment procedure described in Section B of the online supplement. We then use these samples to obtain Monte Carlo approximations of the conditional correlation in (1a) and conditional insurance premium in (3).

4 Simulation Study

In this section, we verify the efficacy of our proposed SQR methodology via a simulation study. It is sufficient to assess the accuracy of the sampling from $g(\tilde{y}, \tilde{p}|\tilde{s})$ for a single state. For $j = 1, \dots, n_t$ and $t = 1, \dots, T$, define that $\tilde{p}_t = \mu_{\tilde{p}}(\tilde{s}_t) + \sigma_{\tilde{p}}(\tilde{s}_t)\epsilon_t^p$, and $\tilde{y}_{jt} = \mu_{\tilde{y}}(\tilde{p}_t, \tilde{s}_t) + \sigma_{\tilde{y}}(\tilde{p}_t, \tilde{s}_t)\epsilon_{jt}^y$, where $\mu_{\tilde{p}}(\tilde{s})$ and $\sigma_{\tilde{p}}(\tilde{s})$ are functions for the conditional mean and standard deviation for \tilde{p}_t , $\mu_{\tilde{y}}(\tilde{p}, \tilde{s})$ and $\sigma_{\tilde{y}}(\tilde{p}, \tilde{s})$ are functions for the conditional mean and standard deviation for \tilde{y}_{jt} , and ϵ_t^p and ϵ_{jt}^y are independent error terms with mean 0 and standard deviation 1. To mimic the sample size from the real corn crop dataset, we assume $n_t = 500$ for $t = 1, \dots, T$ and $T = 100$ throughout the simulation study. We also perform a total of $M = 100$ Monte Carlo iterations of our simulation study. We simulate $\tilde{s}_t \stackrel{iid}{\sim} Beta(7, 44)$ for $t = 1, \dots, T$ where $Beta(\cdot, \cdot)$ is a Beta distribution, chosen to represent the distribution of the observed \tilde{s}_t from the empirical corn crop dataset.

To assess the robustness of our method, we consider both linear and non-linear functional forms for $\mu_{\tilde{p}}(\tilde{s})$ and $\sigma_{\tilde{p}}(\tilde{s})$ as follows:

- Linear mean and standard deviation functions for the harvest price:

$$\mu_{\tilde{p}}(\tilde{s}) = 0.2 - 0.4\tilde{s} \text{ and } \sigma_{\tilde{p}}(\tilde{s}) = 0.5 - 0.5\tilde{s}_t.$$

- Nonlinear mean and standard deviation functions for the harvest price:

$$\mu_{\tilde{p}}(\tilde{s}) = -0.2 + 0.4 \exp(-2\tilde{s}_t) \text{ and } \sigma_{\tilde{p}}(\tilde{s}) = 0.5 \exp(-2\tilde{s}_t).$$

We specify the mean and standard deviation for the yield as:

$$\mu_{\tilde{y}}(\tilde{p}, \tilde{s}) = -25 + 14.45 \exp\{\tilde{p}_t\} + 22.18\tilde{s}_t \text{ and } \sigma_{\tilde{y}}(\tilde{p}_t, \tilde{s}) = 33.$$

The choices of these functions are meant to closely represent the realized detrended corn harvest price and county-level yields in the empirical corn dataset. Due to limited space, results from the linear \tilde{p} configuration are put into the online supplement.

It is commonly observed that the realized detrended harvest price is primarily right skewed, and the detrended crop yields are significantly left skewed (Ker & Tolhurst (2019), Price et al. (2019), Swinton & King (1991), and others). Therefore, we choose to model the error distributions via the skewed normal distribution. The skewed normal distribution, denoted as $X \sim \mathcal{SN}(\mu, \sigma, \alpha)$, has location and scale parameters μ and σ along with an additional skewness parameter, α . When $\alpha > 0$, then the distribution is right skewed and when $\alpha < 0$, then the distribution is left skewed. When $\alpha = 0$, then the distribution is the traditional normal distribution. For this simulation study, we assume that

$$\epsilon_t^p \stackrel{iid}{\sim} \mathcal{SN} \left(- \left(1 - \frac{2d_p^2}{\pi} \right)^{-1/2} d_p \sqrt{\frac{2}{\pi}}, \left(1 - \frac{2d_p^2}{\pi} \right)^{-1/2}, a_p \right), \text{ and} \quad (16)$$

$$\epsilon_{jt}^y \stackrel{iid}{\sim} \mathcal{SN} \left(- \left(1 - \frac{2d_y^2}{\pi} \right)^{-1/2} d_y \sqrt{\frac{2}{\pi}}, \left(1 - \frac{2d_y^2}{\pi} \right)^{-1/2}, a_y \right), \quad (17)$$

for $j = 1, \dots, n_t$, and $t = 1, \dots, T$, where $a_p = 3$, $a_y = -3$, $d_p = \frac{a_p}{\sqrt{1+a_p^2}}$, and $d_y = \frac{a_y}{\sqrt{1+a_y^2}}$.

These specific forms of the location and scale parameters are selected to ensure theoretical errors with zero mean and unit standard deviation. The signs of skew parameters, a_p and a_y , reflect our empirical belief that crop prices are right skewed and crop yields are left skewed.

First, we assess the accuracy of our quantile function estimation. For each Monte Carlo sample ($m = 1, \dots, M$), we estimate \hat{q}_{τ_p} and \hat{q}_{τ_y} for τ_p or $\tau_y \in \{0.1, 0.25, 0.5, 0.75, 0.9\}$, using the methods presented in (12) - (13). More specifically, we calculate $\hat{q}_{\tau_p}(\tilde{s}) = \mathbf{B}^T(\tilde{s})\hat{\boldsymbol{\beta}}_{\tau_p}$ and $\hat{q}_{\tau_y}(\tilde{p}, \tilde{s}) = \mathbf{B}^T(\tilde{p}, \tilde{s})\hat{\boldsymbol{\beta}}_{\tau_y}$ for given \tilde{p} and \tilde{s} where $\mathbf{B}(\tilde{p})$ and $\mathbf{B}(\tilde{s})$ are constructed using $p = 3$ and $K_n = 4$ with compact support $\chi_{\tilde{p}} = [-1, 1]$ and $\chi_{\tilde{s}} = [0, 1]$, representing the range of plausible values of \tilde{p} and \tilde{s} , and $\hat{\boldsymbol{\beta}}_{\tau_p}$ and $\hat{\boldsymbol{\beta}}_{\tau_y}$ are calculated using (14) and (15), respectively. We compare these estimated quantile functions to their true quantile functions, $q_{\tau_p}(\tilde{s}) = \mu_{\tilde{p}}(\tilde{s}) + \sigma_{\tilde{p}}(\tilde{s})q_{\tau_p, \epsilon_{\tilde{p}}}$ and $q_{\tau_y}(\tilde{p}, \tilde{s}) = \mu_{\tilde{y}}(\tilde{p}, \tilde{s}) + \sigma_{\tilde{y}}(\tilde{p}, \tilde{s})q_{\tau_y, \epsilon_{\tilde{y}}}$, where $q_{\tau_p, \epsilon_{\tilde{p}}}$ is τ_p^{th} -quantile of the distribution from (16) and $q_{\tau_y, \epsilon_{\tilde{y}}}$ is τ_y^{th} -quantile of the distribution from (17).

Figure 5 presents the true versus estimated τ_p^{th} -quantile functions for $\tau_p \in \{0.1, 0.25, 0.5, 0.75, 0.9\}$ for non-linear \tilde{p} . For each plot, the solid black line represents the true quantile function, the solid red line represents the median of the M estimated quantile functions, and the dashed red lines represent the 0.025 and 0.975 quantiles of the M estimated quantile functions. Based on the outcome of these graphs, the true quantile functions appears to directly overlap the median of the M estimated quantile functions, and the 0.025 and 0.975 quantile function bands fall close to the true quantile functions, suggesting our method does a good job of approximating the quantile functions of detrended prices \tilde{p} .

We also present the true versus estimated τ_y^{th} - quantile functions for \tilde{y} with $\tau_y \in \{0.1, 0.25, 0.5, 0.75, 0.9\}$ and $\tilde{s} \in \{0.08, 0.103, 0.133, 0.167, 0.201\}$, which are the 0.1, 0.25,

0.5, 0.75, and 0.9 quantiles of the Beta distribution used to simulate \tilde{s}_t . Figure 6 plots the quantiles for \tilde{y} with non-linear \tilde{p} . Again, the true quantile functions are almost identical with the median of the M estimated quantile functions, and the 0.025 and 0.975 quantile function bands fall very close to the true quantile functions, indicating our method can estimate the quantile functions of detrended yields \tilde{y} well.

Recall that the primary objectives of this paper are to estimate the conditional correlation and premium as defined in equations (1a) and (3), respectively. Both of these objectives rely on the ability to sample from the joint density function $g(\tilde{y}, \tilde{p}|\tilde{s})$. Consequently, we proceed to evaluate the performance of our proposed sampling method based on SQR in estimating the joint distribution $g(\tilde{y}, \tilde{p}|\tilde{s})$.

For this evaluation, we consider $\tilde{s} \in \{0.103, 0.133, 0.167\}$, which are the 0.25, 0.5, and 0.75 quantiles of the Beta distribution used to simulate \tilde{s}_t . For each \tilde{s} , we simulate R pairs $\{\tilde{p}_r^*, \tilde{y}_r^*\}_{r=1}^R$ based on their estimated quantile functions. Using these samples, we then estimate the 2-d density $\hat{g}(\tilde{y}, \tilde{p}|\tilde{s})$ using the R function `kde2d` in the `MASS` package (Venables & Ripley (2002)). We compare the estimated density function \hat{g} to the “true” density function g where

$$\begin{aligned}
g(\tilde{y}, \tilde{p}|\tilde{s}) &= g(\tilde{y}|\tilde{p}, \tilde{s})g(\tilde{p}|\tilde{s}) \\
&= \frac{1}{\sigma_{\tilde{y}}(\tilde{p}, \tilde{s})} g\left(\frac{\tilde{y} - \mu_{\tilde{y}}(\tilde{p}, \tilde{s})}{\sigma_{\tilde{y}}(\tilde{p}, \tilde{s})} \middle| \tilde{p}, \tilde{s}\right) \frac{1}{\sigma_{\tilde{p}}(\tilde{s})} g\left(\frac{\tilde{p} - \mu_{\tilde{p}}(\tilde{s})}{\sigma_{\tilde{p}}(\tilde{s})} \middle| \tilde{s}\right) \\
&= \frac{1}{\sigma_{\tilde{y}}(\tilde{p}, \tilde{s})} g(\epsilon^y|\tilde{p}, \tilde{s}) \frac{1}{\sigma_{\tilde{p}}(\tilde{s})} g(\epsilon^p|\tilde{s})
\end{aligned} \tag{18}$$

where $g(\epsilon^p|\tilde{s})$ and $g(\epsilon^y|\tilde{p}, \tilde{s})$ are the density functions of the distributions from (16), and (17), respectively. Figure 7 illustrates the comparisons, demonstrating that the estimated density obtained from our draws closely aligns with the true joint densities, even when viewed from different angles. We further perform a 2-dimensional Kolmogorov-Smirnov test, as proposed

in Fasano & Franceschini (1987), on all 100 Monte Carlo samples to assess the agreement between these two bivariate densities. The average p-values across the 100 samples are 0.25, 0.36, and 0.46 for $\tilde{s} = 0.103, 0.133, 0.1767$ respectively. These relatively large p-values, combined with the visual comparisons in Figure 7, indicate that our SQR-based sampling method effectively generates valid samples from the target joint price and yield density.

In summary, the results of the simulation study conducted in this section affirm the efficacy of our SQR with penalized B-spline method in generating sample draws that accurately estimate the true joint price and yield density.

5 Empirical Study

In this section, we utilize our method to generate samples from both the stock-conditioned joint density $g(\tilde{y}, \tilde{p}|\tilde{s})$ and the unconditional joint density $g(\tilde{y}, \tilde{p})$, which is independent of stocks. These samples are then employed to compute the crop insurance premium and the correlation between harvest price and county-level yield. The methodology of sampling from $g(\tilde{y}, \tilde{p})$ is a special case of our sampling methodology from $g(\tilde{y}, \tilde{p}|\tilde{s})$, and such details are provided in Appendix C of the on-line supplement. For this data analysis, we obtain harvest time price (in U.S.\$ per bushel) for corn and soybeans, both national-level yield and stocks for corn and soybeans, and state and county-level yields from twelve U.S. states which are considered to be part of the “corn belt” (Illinois, Indiana, Iowa, Kansas, Michigan, Minnesota, Missouri, Nebraska, North Dakota, Ohio, South Dakota, and Wisconsin) from the years 1990 to 2018 (i.e., $T = 29$). Note that each state has a different number of counties, and not every county has a reported yield in each year (i.e., n_t is different for $t = 1, \dots, T$). In

total, we have 29 observed values of p_t and \tilde{s}_t for $t = 1, \dots, T$ for both corn and soybeans, and 27,937 and 25,946 observed values of y_{jt} for corn and soybeans, respectively, $t = 1, \dots, T$, and $j = 1, \dots, n_t$. For each state, we apply the detrending procedures outlined in (8) and (11) to obtain \tilde{p}_t and \tilde{y}_{jt} for $t = 1, \dots, T$ and $j = 1, \dots, n_t$. These detrended values are then utilized in our SQR methodology to generate samples $\{\tilde{y}_r^*, \tilde{p}_r^*\}_{r=1}^R$ from both $g(\tilde{y}_{jt}, \tilde{p}_t | \tilde{s}_t)$ and $g(\tilde{y}_{jt}, \tilde{p}_t)$, respectively. We then apply our retrending procedure from Section B of the online supplement to obtain samples from $\{y_{2020,r}^*, p_{2020,r}^*\}_{r=1}^R$ from both $g(y_{2020,jt}, p_{2020,t} | \tilde{s}_t)$ and $g(y_{2020,jt}, p_{2020,t})$. The tuning parameters p , K_n , and λ are selected following the same approach as in the simulation study. For the empirical data study, we set $R = 5000$. The corn and soybean results are empirically similar, so we only present the corn results in this paper and the soybean results can be found in Appendix E of the on-line supplement.

Figure 8 presents the estimated standard deviation of \tilde{p} across different levels of stocks from the conditional density function represented by a solid black line. For comparison, we also plot the estimated unconditional standard deviation as a dashed red line. Since the estimated trend \hat{p}_t eliminates any yearly patterns in the price dataset, the samples from $g(\tilde{p}_t | \tilde{s}_t)$ are employed to empirically estimate the relationship between stocks and the volatility of the harvest price. As discussed in the introduction, we want to understand the relationship between stocks and price variability to help understand the source of large spikes in commodity priced. We observe that the conditional standard deviation tends to decrease as level of stocks increases, as theorized in (2), suggesting that large and dramatic price spikes are more likely for low levels of stock, and tends to become less likely as stocks increase.

Figure 9 plots visualizations of the impact of stocks on the correlation between the

harvest time price and county-level yields (in 2020 units) for the corn in each of the twelve states. In addition to the estimates of the conditional correlations as functions of stocks (represented by the black solid curve), we display a 95% confidence band for the conditional correlation estimate, shown as black dotted lines. The standard error of the estimated conditional standard deviation is computed using a Jackknife delete-a-group method with $B = 50$ groups. More specifically, within each state, we order the data points by year and by county, and systematically assign price-yield pairs to form a Jackknife group. Much as we had initially theorized in (1a), both the unconditional and conditional correlations for corn are negative, suggesting that when we observe a negative shock in yield for a given year, then we should expect a subsequent increase in the harvest price. In addition, we observe a rise in the conditional correlation as the level of stock increases for a majority of states, providing evidence that as the level of stocks/storage increases, correlation also increases, as is theorized in (1b). This also suggests that the shift in the demand curve for high levels of storage for corn as illustrated in Figure 2 is realized empirically.

The “I” states – Illinois, Indiana, and Iowa, widely understood as the core production region of corn, and displayed in the top panel of Figure 9 – as well as southern states like Missouri and Ohio appear to exhibit similar trends of the conditional correlation relative to the unconditional correlation for corn; that is the conditional correlation is significantly lower than the unconditional correlation for low levels of stock and increases as stock increases. However, states to the north of the core production region such as Michigan, Minnesota, North Dakota, and Wisconsin exhibit conditional correlation curves that are flatter relative to the curves of the “I” states, Missouri, and Ohio, and do not appear to be significantly different than the unconditional correlation. In addition, the levels of conditional correla-

tion are comparatively much smaller in magnitude for these outside states for corn. This empirically illustrates the natural hedge proposed in the introduction, whereby states in the core production areas have the regional competitive advantage that current-year yield and harvest price are highly negatively correlated when carryover stocks are low, keeping revenue in those regions stable. In regions going away from the center of production, we see that yield and price correlation is less sensitive to changes in the amount of carryover stocks, meaning revenue could end up in a shortfall in these areas, leading to a competitive disadvantage. This regional competitive advantage can also be seen in Figure 10, where we present the conditional correlations as geographic heat maps for the observed 0.2-, 0.5-, and 0.8-quantiles of leftover stocks for corn, where the states displaying darker shades of red represents states with more negative price-yield correlations.

We further illustrate the natural hedge through estimation of the conditional insurance premium, hereafter referred to as the proposed insurance premium, as defined in (3). We compare the conditional insurance premiums from our proposed methodology to insurance premiums using current USDA methodologies. Using our samples $\{y_{2020,r}^*, p_{2020,r}^*\}_{r=1}^R$ from $g(y_{2020,jt}, p_{2020,t} | \tilde{s}_t)$, we approximate the proposed insurance premium as

$$\frac{1}{R} \sum_{r=1}^R \max(\psi \bar{p}_t \bar{y}_t - p_r^* y_r^*, 0). \quad (19)$$

The USDA's Risk Management Agency (RMA) uses commodity market's futures implied volatilities in determining the harvest price distribution, where market traders are influenced by current levels of stocks. However, the RMA does not take into account the current level of stocks when determining the distribution of crop yields; nor does the RMA take into account stocks when calculating the price-yield correlation. To simulate the current RMA procedure,

based on a bivariate copula, we import our samples $\mathbf{p}^* = \{p_r^*\}_{r=1}^R$ from $g(p_{2020,t}|\tilde{s}_t)$, the conditional distribution, and $\mathbf{y}^* = \{y_r^*\}_{r=1}^R$ from $g(y_{2020,jt})$, the unconditional distribution, and perform the following:

1. Set $\gamma = \hat{\text{c\`{o}r}}(p_{2020,t}, y_{2020,jt})$, the estimated unconditional price-yield correlation.
2. For r in 1 to R :
 - Simulate $\begin{bmatrix} \epsilon_r^p \\ \epsilon_r^y \end{bmatrix} \sim \mathcal{N}\left(\begin{bmatrix} 0 \\ 0 \end{bmatrix}, \begin{bmatrix} 1 & \gamma \\ \gamma & 1 \end{bmatrix}\right)$.
 - Set $\tau_r^p = \Phi(\epsilon_r^p)$; $\tau_r^y = \Phi(\epsilon_r^y)$, where Φ represents the cdf of the standard normal.
 - Set p_r^+ to be the τ_r^p quantile of \mathbf{p}^* and y_r^+ to be the τ_r^y quantile of \mathbf{y}^*

End For

3. Calculate an approximation of the county-level premium in (3) as

$$\frac{1}{R} \sum_{r=1}^R \max(\psi \bar{p}_t \bar{y}_t - p_r^+ y_r^+, 0). \quad (20)$$

We use the approximations of the county-level premiums as imputations of the current methodology insurance premiums.

The differences in the computed insurance premiums between our proposed method in (19) and the imputed current method in (20) are illustrated in Figure 11, considering a coverage level of $\psi = 0.7$, plotted across different levels of \tilde{s}_t . We assume that \bar{p}_t is the year t spring future's price and \bar{y}_t is the 2020-adjusted arithmetic average of the past ten years of yield data broken down by state. In addition to the estimates of the differences of insurance premiums (represented by the black solid curve), we display a 95% confidence band for the premium difference estimates, shown as black dotted lines, using the same Jackknife groups as discussed previously.

We previously noted that the ‘‘I’’ states as well as Missouri and Ohio have conditional price-yield correlation for low levels of stock for corn that is significantly more negative than

the unconditional correlation. For these states, when stocks are low and the unconditional correlation is inserted rather than the conditional correlation, then harvest revenue ($p_t y_{jt}$) will be modeled as being more variable than they actually are because less negative levels of correlation are likely less effective in stabilizing revenue. Thus, the difference between the proposed method and the imputed current methodology is expected to be negative, which is can be seen in Figure 11, aside from Indiana.

For the northern states such as Michigan, Minnesota, North Dakota, and Wisconsin, we observe no significant difference between the conditional and unconditional correlation for corn at these low levels of stock in Figure 9. Subsequently, we observe no significant difference in the proposed and imputed current premiums for low levels of stock for these states, except for Michigan, in Figure 11. The lone exception to these observations is the spike in premium differences at $\tilde{s}_t = 0.075$, representing the calendar year 2012, which was a drought year, and negative affected yields in the states in the core region more than the states to the north. In general the cooler northern states, and also Kansas and Nebraska where extensive irrigation supplements rainfall, display patterns in conditional correlation that are least typical. Crop production in these states are least susceptible to drought, the primary reason for production shortfall.

We also note that the “I” states as well as Kansas, Missouri, and Ohio have conditional price-yield correlations for high levels of stock that are larger than the unconditional correlation for corn. Using similar rationale stated previously, inserting the unconditional correlation instead of the conditionl correlation means harvest revenue ($p_t y_{jt}$) will be modeled as being less variable than they actually are. Thus, the difference between the proposed method and the imputed current methodology would be positive, which is seen in Figure 11.

For the previously mentioned northern states, we observe no significant difference between the conditional and unconditional correlation for corn at these high levels of stock in Figure 9, and thus, no significant difference in the proposed and imputed current premiums for low levels of stock for these states in Figure 11.

We point out that the effect of stocks has already been partially factored into the RMA premium calculation through the real-time implied volatility that the RMA obtains from options markets, which we account for in our imputation method through the conditional density $g(\tilde{p}_t|\tilde{s}_t)$. Therefore, we might expect to observe insignificant differences between the imputed current and proposed premiums for levels of stock where the differences between conditional and unconditional correlations are not large. For values of \tilde{s}_t between 0.10 and 0.20 for corn, we do observe such an insignificant difference of insurance premiums between our proposed and the imputed current RMA methodologies. We note that our proposed methodology does not take into account any innovations in actuarial rate setting procedures as well as global economic trends, which may also account for any observed differences in Figure 11. On the whole, while further inquiry is warranted, our sense is that the current approach to premium setting does a good job for typical levels of stock, gives premiums that are somewhat lower than is warranted when stocks are very high and may be off in either direction when stocks are low.

6 Conclusion

We address whether the inclusion of stocks has a significant impact on correlation between yield and harvest price in the U.S. Corn and soybean markets as well as RI premiums. To

answer these questions, we obtain samples from the unconditional joint density function $g(y_{jt}, p_t)$ and the conditional joint density function $g(y_{jt}, p_t | \tilde{s}_t)$ using SQR with penalized B-splines and then use these samples to obtain approximations for both the correlation and county-level insurance premiums. Our SQR methodology to approximate a joint price-yield density is novel, but necessary to accurately estimate the price-yield correlation and revenue insurance premiums. We obtain these samples using county-level yield data and national-level yield, stocks, and price data from both corn and soybean crops across 12 “corn belt” states from 1990 to 2018. We observe that lower stocks imply a more significantly negative correlation between yield and price, and also that higher levels of stock typically mean a less negative correlation.

We obtain approximations of the conditional and unconditional correlations broken down by states. We observe that the core cornbelt “I” states are more pronounce in how correlation becomes less negative as stocks increase. However, we observe that most of the other states, in the periphery, do not reveal a significant difference between the conditional and unconditional stocks for the differing levels of stock. We also obtain approximations of the state-level insurance premiums, using a simulation of the currently imposed methodology as well as our proposed method conditioning on stocks. We observe that the “I” states, which have significantly different approximations for the conditional correlation compared to the unconditional correlation, tend to misspecify the current county-level insurance premiums compared to premiums from our proposed methodology for both small and large levels of stocks. In addition, we observe that states in the periphery tend to have a insignificant premium difference using our proposed methodology compared to the imputed current RMA methodology for all levels of stocks.

References

- Barnwal, P. & Kotani, K. (2013). Climatic impacts across agricultural crop yield distributions: An application of quantile regression on rice crops in Andhra Pradesh, India. *Ecological Economics*, 87, 95–109.
- Bellemare, M. F., Barrett, C. B., & Just, D. R. (2013). The welfare impacts of commodity price volatility: Evidence from rural Ethiopia. *American Journal of Agricultural Economics*, 95(4), 877–899.
- Black, F. (1976). The pricing of commodity contracts. *Journal of Financial Economics*, 3(1-2), 167–179.
- Blair, G., Christensen, D., & Rudkin, A. (2021). Do commodity price shocks cause armed conflict? A meta-analysis of natural experiments. *American Political Science Review*, 115(2), 709–716.
- Cai, J., de Janvry, A., & Sadoulet, E. (2020). Subsidy policies and insurance demand. *American Economic Review*, 110(8), 2422–53.
- Cariappa, A., Mahida, D., Lal, P., & Chandel, B. (2021). Correlates and impact of crop insurance in India: Evidence from a nationally representative survey. *Agricultural Finance Review*, 81(2), 204–221.
- Chambers, R. (1989). Insurability and moral hazard in agricultural insurance markets. *American Journal of Agricultural Economics*, 74(3), 646–654.
- Chen, S. & Yu, C. L. (2016). Parameter estimation through semiparametric quantile regression imputation. *Electronic Journal of Statistics*, 10(2), 3621 – 3647.
- Chen, Z., Dall’erba, S., & Sherrick, B. J. (2020). Premium misrating in federal crop insurance programs: scale, geography, and fiscal impacts. *Agricultural Finance Review*, 80(5), 693–713.
- Coble, K., Knight, T., Goodwin, B., Miller, M., & Rejesus, R. (2010). A comprehensive review of the rma aph and combo rating methodology final report.
- de Boor, C. (1978). *A Practical Guide to Splines*, volume 27. Applied Mathematical Sciences, New York: Springer, 1978.
- De Winne, J. & Peersman, G. (2021). The impact of food prices on conflict revisited. *Journal of Business & Economic Statistics*, 39(2), 547–560.
- Deaton, A. & Laroque, G. (1992). On the behaviour of commodity prices. *The Review of Economic Studies*, 59(1), 1–23.
- Du, X., Feng, H., & Hennessy, D. (2017). Rationality of choices in subsidized crop insurance markets. *American Journal of Agricultural Economics*, 99(3), 732–756.

- Fasano, G. & Franceschini, A. (1987). A multidimensional version of the Kolmogorov–Smirnov test. *Monthly Notices of the Royal Astronomical Society*, 225(1), 155–170.
- Finger, R. (2012). *How strong is the “natural hedge”? The effects of crop acreage and aggregation levels*. 123rd Seminar, February 23-24, 2012, Dublin, Ireland 122538, European Association of Agricultural Economists.
- Gardner, B. L. (2002). *American Agriculture in the Twentieth Century: How It Flourished and What It Cost*. Cambridge, MA: Harvard University Press.
- Gong, X., Hennessy, D., & Feng, H. (2023). Systemic risk, relative subsidy rates and area yield insurance choice. *American Journal of Agricultural Economics*, in press.
- Goodwin, B. K. (2001). Problems with market insurance in agriculture. *American Journal of Agricultural Economics*, 83(3), 643–649.
- Goodwin, B. K. & Ker, A. P. (1998). Nonparametric estimation of crop yield distributions: Implications for rating group-risk crop insurance contracts. *ERN: Nonparametric Methods (Topic)*, 80(1), 139–153.
- Hennessy, D. A. & Wahl, T. I. (1996). The effects of decision making on futures price volatility. *American Journal of Agricultural Economics*, 78(3), 591–603.
- Innes, R. (2003). Crop insurance in a political economy: an alternative perspective on agricultural policy. *American Journal of Agricultural Economics*, 85(2), 318–335.
- Just, R., Calvin, L., & Quiggin, J. (1999). Adverse selection in crop insurance: Actuarial and asymmetric information incentives. *American Journal of Agricultural Economics*, 81(4), 834–849.
- Karali, B. & Power, G. J. (2013). Short- and long-run determinants of commodity price volatility. *American Journal of Agricultural Economics*, 95(3), 724–738.
- Ker, A. P. & Coble, K. (2003). Modeling conditional yield densities. *American Journal of Agricultural Economics*, 85(2), 291–304.
- Ker, A. P. & Tolhurst, T. N. (2019). On the Treatment of Heteroscedasticity in Crop Yield Data. *American Journal of Agricultural Economics*, 101(4), 1247–1261.
- Koenker, R. (2000). Galton, Edgeworth, Frisch, and prospects for quantile regression in econometrics. *Journal of Econometrics*, 95(2), 347–374.
- Koenker, R. & Bassett, G. (1978). Regression quantiles. *Econometrica*, 46(1), 33–50.
- Koenker, R. & Hallock, K. F. (2001). Quantile regression. *Journal of Economic Perspectives*, 15(4), 143–156.
- Koenker, R., Ng, P., & Portnoy, S. (1994). Quantile smoothing splines. *Biometrika*, 81(4), 673–680.

- Kramer, B., Hazell, H., Alderman, H., Ceballos, F., Kiumar, N., & Timu, A. (2022). Is agricultural insurance fulfilling its promise for the developing world? a review of recent evidence. *Annual Review of Resource Economics*, 14(9), 1–21.
- Liao, W.-C. & Wang, X. (2012). Hedonic house prices and spatial quantile regression. *Journal of Housing Economics*, 21(1), 16–27.
- Ming, W., Shi, P., & Te, Y. (2016). Factors affecting farmers' crop insurance participation in China. *Canadian Journal of Agricultural Economics*, 64(3), 479–492.
- Oi, W. Y. (1961). The desirability of price instability under perfect competition. *Econometrica*, 29(1), 58–64.
- Price, M., Yu, C., Hennessy, D., & Du, X. (2019). Are actuarial crop insurance rates fair?: an analysis using a penalized bivariate b-spline method. *Journal of the Royal Statistical Society*, 68(5), 1207–1232.
- Puga, D. (2010). The magnitude and causes of agglomeration economies. *Journal of Regional Science*, 50(1), 203–219.
- Ramirez, O. & Carpio, C. (2012). Premium estimation inaccuracy and the actuarial performance of the US crop insurance program. *Agricultural Finance Review*, 72(1), 117–133.
- Ramirez, O. A. & Shonkwiler, J. S. (2017). A Probabilistic Model of Crop Insurance Purchase Decision. *Journal of Agricultural & Resource Economics*, 42(1), 1–17.
- Ramsey, A. F. (2020). Probability distributions of crop yields: A bayesian spatial quantile regression approach. *American Journal of Agricultural Economics*, 102(1), 220–239.
- Ramsey, A. F., Goodwin, B. K., & Ghosh, S. (2019). How high the hedge: Relationships between prices and yields in the federal crop insurance program. *Journal of Agricultural & Resource Economics*, 44(2), 227–245.
- Santeramo, F. & Ramsey, A. (2017). Crop insurance performance by crop persists over time. *farmdoc daily*, 12(110).
- Schnitkey, G., Paulson, N., Zulauf, C., Swanson, K., Colussi, J., & Baltz, J. (2022). Nitrogen fertilizer prices and supply in light of the Ukraine-Russia conflict. *farmdoc daily*, (45).
- Smith, V. & Glauber, J. (2019). The future of US farm policy. *EuroChoices*, 18(1), 42–48.
- Stüttgen, P., Boatwright, P., & Kadane, J. B. (2018). Stockouts and restocking: Monitoring the retailer from the supplier's perspective. *Journal of Business & Economic Statistics*, 36(3), 471–482.
- Swinton, S. M. & King, R. P. (1991). Evaluating Robust Regression Techniques for Detrending Crop Yield Data with Nonnormal Errors. *American Journal of Agricultural Economics*, 73(2), 446–451.

- Ten, K. S. & Zhang, J. (2023). Flexible weather index insurance design with penalized splines. *North American Actuarial Journal*, *in press*.
- Turnovsky, S. J., Shalit, H., & Schmitz, A. (1980). Consumer's surplus, price instability, and consumer welfare. *Econometrica*, 48(1), 135–152.
- Venables, W. N. & Ripley, B. D. (2002). *Modern Applied Statistics with S*. New York: Springer, fourth edition. ISBN 0-387-95457-0.
- Yoshida, T. (2022). Asymptotics for penalized spline estimators in quantile regression. *Communications in Statistics - Theory & Methods*, 0(0), 1–20.
- Yu, K. & Jones, M. C. (1998). Local linear quantile regression. *Journal of the American Statistical Association*, 93(441), 228–237.
- Yuan, M. (2006). Gacv for quantile smoothing splines. *Comput. Stat. Data Anal.*, 50, 813–829.
- Zimmer, D. M. (2012). The role of copulas in the housing crisis. *The Review of Economics & Statistics*, 94(2), 607–620.

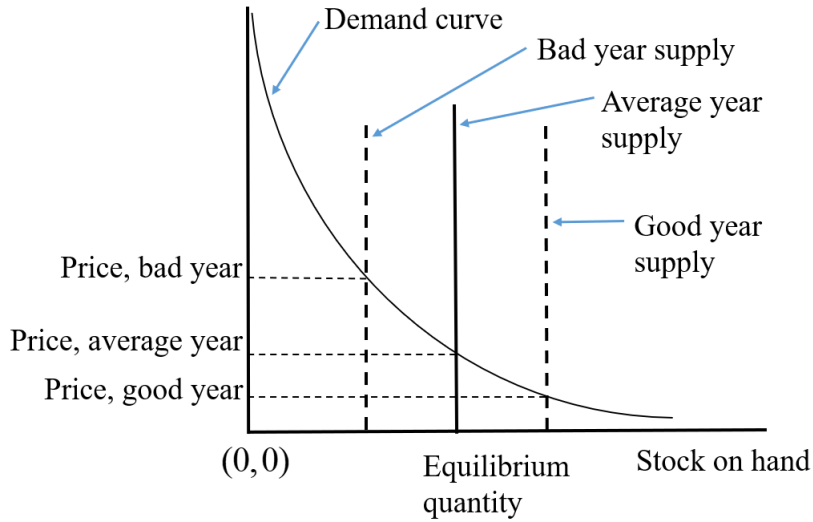


Figure 1: Demand curve and equilibrium price for a crop of interest when stocks are not incorporated in the demand curve.

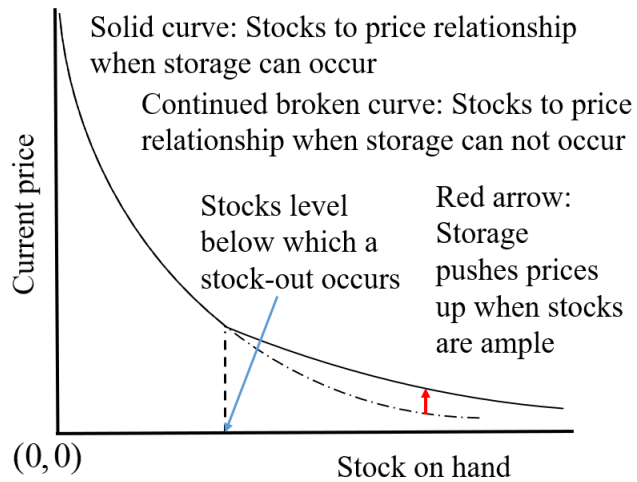


Figure 2: Demand curve and equilibrium price for a crop of interest with the inclusion of stocks in the demand curve.

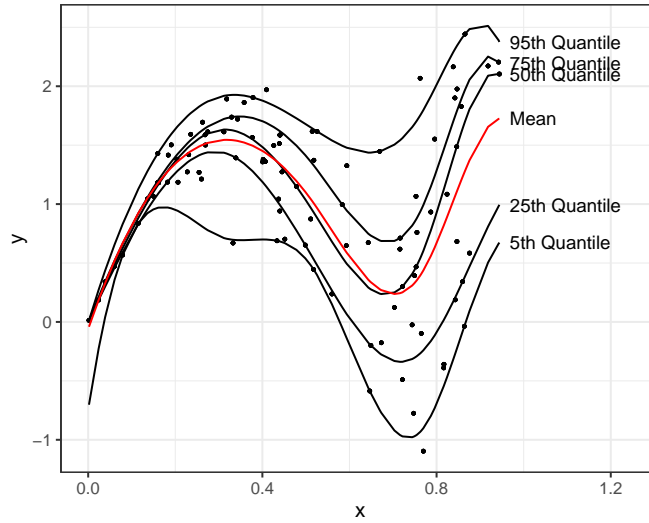


Figure 3: Illustration of Semi-parametric Quantile Regression for a general density $g(y|x)$. Here, the black curves represent the SQR estimates of the 0.05th-, 0.25th-, 0.5th-, 0.75th-, and 0.95th-quantile curves and the red line represents the regression mean, estimated semi-parametrically.

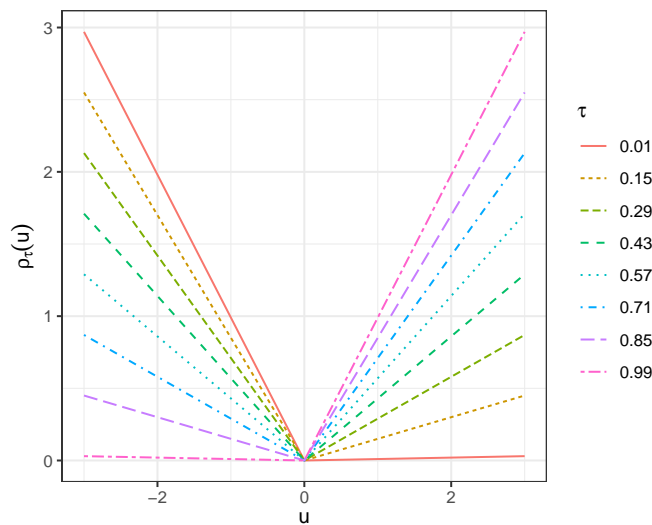


Figure 4: Illustration of the check loss function $\rho_\tau(u) = u(\tau - I(u < 0))$ used in quantile regression for eight different values of τ equally spaced between 0.01 and 0.99.

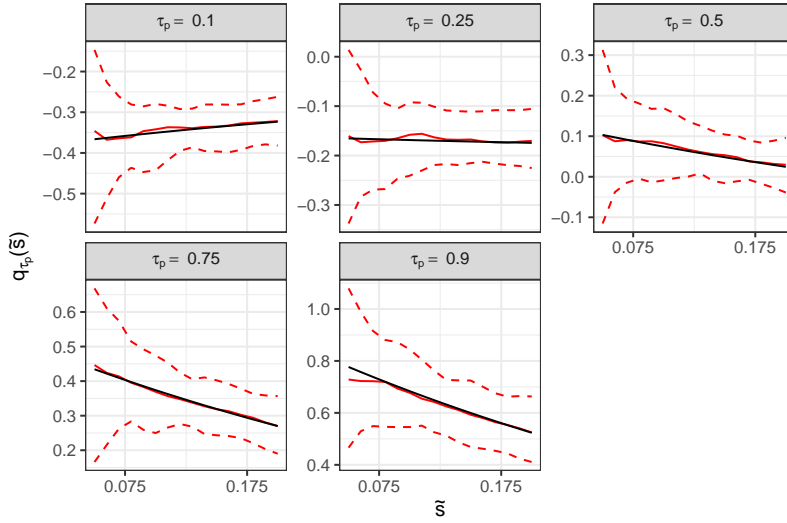


Figure 5: True and estimated quantile functions of \tilde{p} from the non-linear \tilde{p} simulation study. Presented are the medians (solid red lines) and 0.025 and 0.975 quantiles (dashed red lines) of the MC estimates for the quantile regression function $q_{\tau_p}(\tilde{s}_t)$ against the associated true quantile curve (solid black lines). Each plot represents a different $\tau_p \in \{0.1, 0.25, 0.5, 0.75, 0.9\}$.

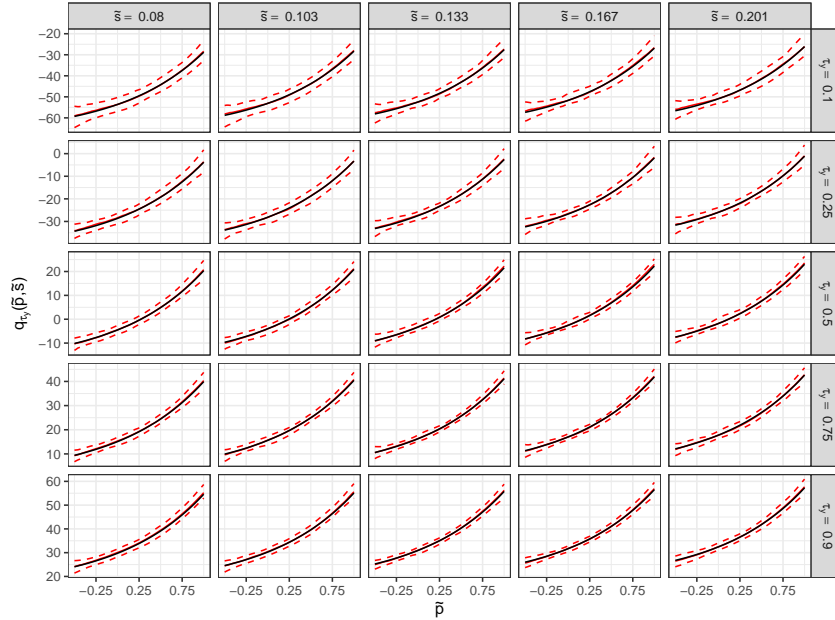


Figure 6: True and estimated quantile functions of \tilde{y} from the non-linear \tilde{p} and linear \tilde{y} simulation study. Presented are the medians (solid red lines) and 0.025 and 0.975 quantiles (dashed red lines) of the MC estimates for the quantile regression function $q_{\tau_y}(\tilde{p}_t, \tilde{s}_t)$ against the associated true quantile curve (solid black lines). Each row represents a different $\tau_y \in \{0.1, 0.25, 0.5, 0.75, 0.9\}$ and each column represents the $\{0.1, 0.25, 0.5, 0.75, 0.9\}$ quantiles of the distribution of \tilde{s} .

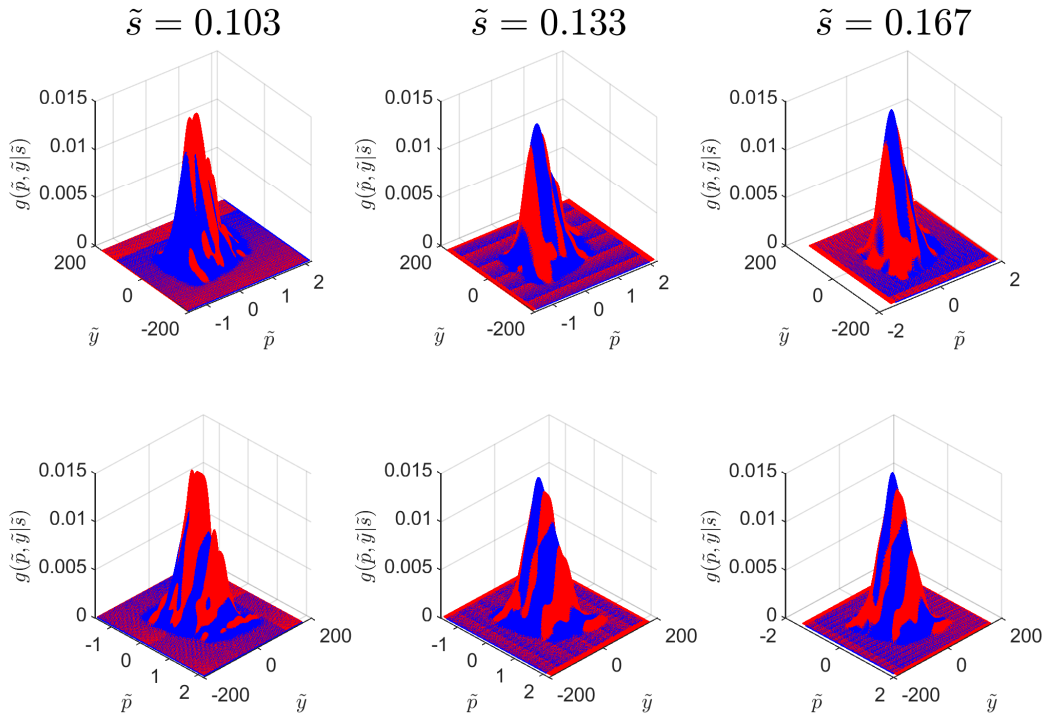


Figure 7: 3d kernel density plots for the approximate joint density $\hat{g}(\tilde{y}, \tilde{p} | \tilde{s})$ in red and the true joint density $g(\tilde{y}, \tilde{p} | \tilde{s})$ in blue for the non-linear \tilde{p} and non-linear \tilde{y} simulation study. Each column represents a different value of $\tilde{s} \in \{0.103, 0.133, 0.167\}$ and each row represents a different viewing angle of the plot.

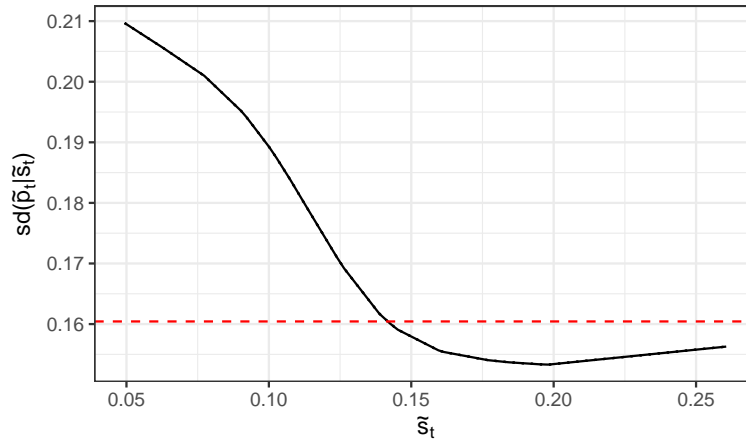


Figure 8: Standard deviation of harvest price as function of stocks for corn crops from 1990-2018 (in 2020 units). The dashed red line is the estimate of the unconditional standard deviation and the solid black line is the estimate of the conditional standard deviation function.

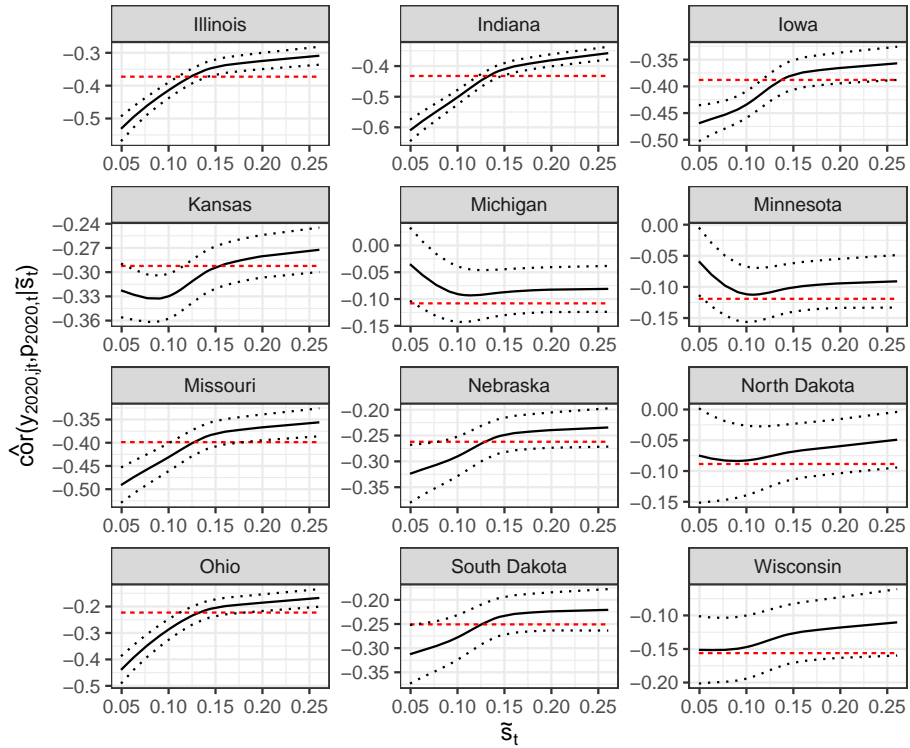


Figure 9: Correlation of harvest price and county-level yield as function of stocks for corn crops by state from 1990-2018 (in 2020 units). The dashed red line is the estimate of the unconditional correlation, the solid black line is the estimate of the conditional correlation function, and the dotted black lines are the 95% confidence bands for the conditional correlation function.

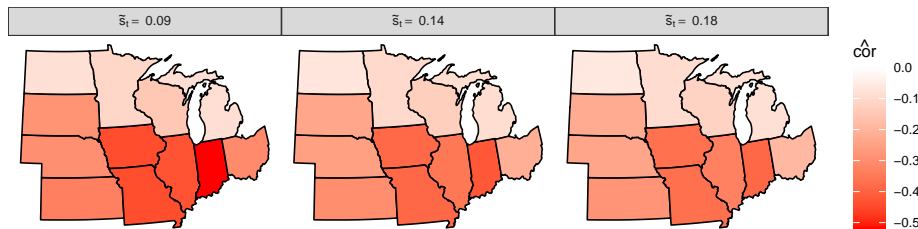


Figure 10: Heat map of the conditional correlation of harvest price and county-level yield for corn crops across states for the observed 0.2- (left panel), 0.5- (middle panel), and 0.8- (right panel) quantiles of leftover stocks. Darker shades of red represent states with more negative correlation.

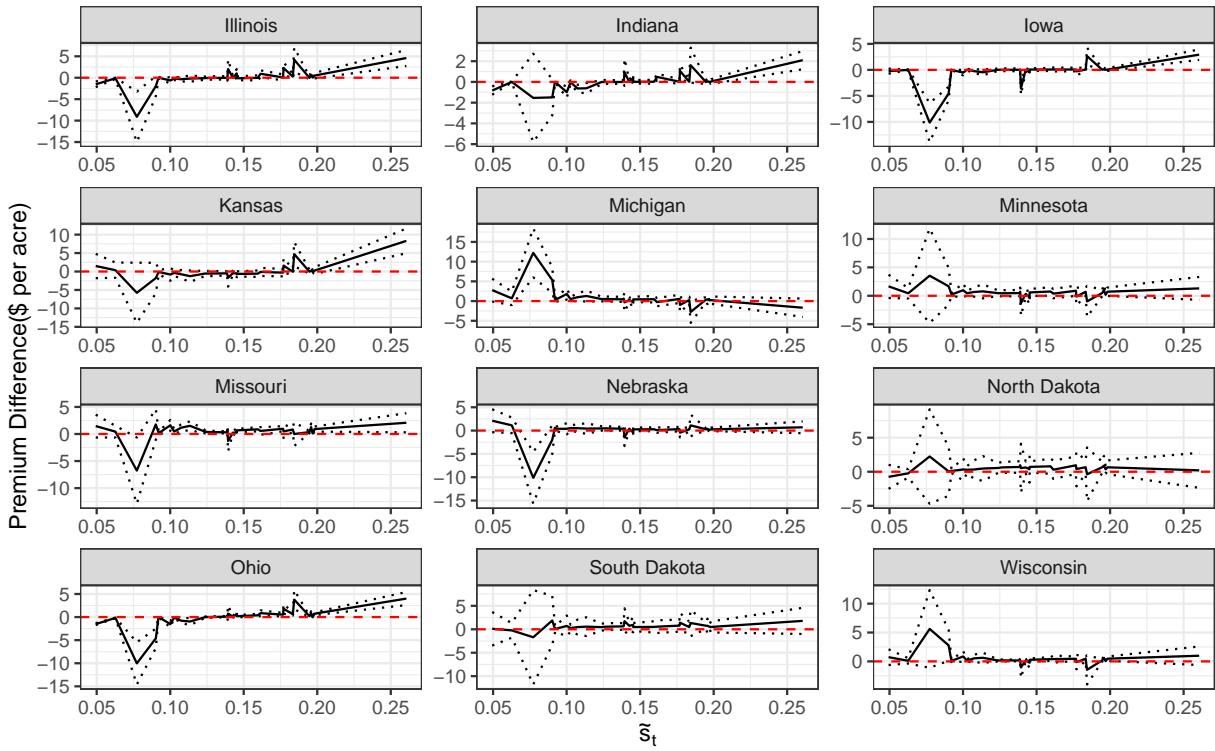


Figure 11: Estimated difference in the proposed insurance premium and the imputed current insurance premium ($\psi = 0.7$) for corn crops by state from 1990-2018 (in 2020 units). The dashed red line is a reference line at 0, and the gray shaded area is a reference for when spring future's price rose significantly.

Online Supplement for “The Impact of Stocks on Correlations of Crop Yields and Prices and on Revenue Insurance Premiums using Semiparametric Quantile Regression with Penalized B-splines”

This online supplement provides additional details about the methodology and simulation results discussed in the main text of “The Impact of Stocks on Correlations of Crop Yields and Prices and on Revenue Insurance Premiums using Semiparametric Quantile Regression with Penalized B-splines”

A B-spline basis formation

The B-spline basis functions, $\mathbf{B}(x)$ for a generic continuous variable, x with degree p and number of knots $K_n - 1$ is constructed as follows: First, recall that $x \in \chi$ and let us further define $\chi = [l_x, u_x]$ where l_x and u_x are the lower and upper bounds for values of x . In order to construct the B-spline basis, we must define knots as κ_k for $k = -p, -p + 1, \dots, K_n + p - 1, K_n + p$ where

$$\kappa_k = \begin{cases} q_{k/K_n} & 1 \leq k \leq K_n - 1 \\ l_x & k \leq 0 \\ u_x & k \geq K_n \end{cases}$$

with q_{k/K_n} being the $\frac{k}{K_n}$ th-quantile of the observed values x_1, x_2, \dots, x_n .

The p^{th} B-spline basis function is then constructed as

$$\mathbf{B}(x) = \left\{ B_{-p+1}^{[p]}(x), B_{-p+2}^{[p]}(x), \dots, B_{K_n}^{[p]}(x) \right\}' \quad (\text{A.1})$$

where $B_k^{[p]}(x)$ for $k = -p + 1, \dots, K_n$ are defined recursively as follows.

For $s = 0$,

$$B_k^{[0]}(x) = \begin{cases} 1 & \kappa_{k-1} < x \leq \kappa_k \\ 0 & \text{otherwise} \end{cases}, \text{ where } k = -p + 1, \dots, K_n + p.$$

For $s = 1, 2, \dots, p$,

$$B_k^{[s]}(x) = \frac{x - \kappa_{k-1}}{\kappa_{k+s-1} - \kappa_{k-1}} B_k^{[s-1]}(x) + \frac{\kappa_{k+s} - x}{\kappa_{k+s} - \kappa_k} B_{k+1}^{[s-1]}(x),$$

where $k = -p + 1, \dots, K_n + p - s$.

B Inflation Adjustment Procedure

Recall from the main text, we set \tilde{p}_t to be the difference between year t 's log-harvest price and a regression estimate of the log harvest price. More specifically, we set $\tilde{p}_t = \log(p_t) - \hat{p}_t$, where \hat{p}_t is a regression estimate of $\log(p_t)$ using localized estimated scatterplot smoothing (LOESS) regressed on year t . In addition, for y_{jt} , we perform a penalized B-spline regression for mean yearly crop yield by state where \hat{y}_{cjt} is the year t regression estimate, or trend,

for state c_j and the detrended county-level yield, \tilde{y}_{jt} , is $\tilde{y}_{jt} = y_{jt} - \hat{y}_{c_j t}$. This section of the online supplement will discuss the methods of going from year t 's detrended price and yield $(\tilde{p}_t, \tilde{y}_{jt})$, into year t 's price and yield expressed in 2020 units $(\tilde{p}_{2020,t}, \tilde{y}_{2020,jt})$.

For p_t , we account for inflation by dividing p_t by the GDP deflator, which measures the changes in prices for all the goods and services produced in an economy. The GDP deflator for year t is defined as $GDPDEF_t = \frac{Nominal_t}{Real_{2020,t}}$, where $Nominal_t$ is the U.S. Nominal GDP in year t and $Real_{2020,t}$ is the U.S. Real GDP in year t expressed in 2020 dollars. Thus, we can obtain $p_{2020,t}$ as

$$p_{2020,t} = \frac{p_t}{GDPDEF_t}. \quad (\text{B.1})$$

We also need to adjust the county-level yield to be expressed in 2020 units. To go from \tilde{y}_{jt} to y_{jt} , we add back $\hat{y}_{c_j t}$, the estimate of annual crop yield in year t in state c_j . So, to obtain the county-level yield in 2020 units, we should add in $\hat{y}_{c_j,2020}$ instead. Thus,

$$\begin{aligned} y_{2020,jt} &= \hat{y}_{c_j,2020} + \tilde{y}_{jt} \\ &= y_{jt} + \hat{y}_{c_j,2020} - \hat{y}_{c_j t}. \end{aligned} \quad (\text{B.2})$$

C Sampling procedure for the unconditional joint distribution

We utilize a similar procedure to obtain samples from the unconditional density $g(y_{2020}, p_{2020}) = g(p_{2020})g(y_{2020}|p_{2020})$. Because the univariate density for \tilde{p} is not dependent on any other variables, the τ_p^{th} -quantile is no longer a function, and we only need to estimate the quantile scalar q_{τ_p} in addition to the quantile function $q_{\tau_y}(\tilde{p})$. In other words, for each state we have

$$\hat{q}_{\tau_p} = \hat{\beta}_{\tau_p} \quad \text{and} \quad (\text{C.1})$$

$$\hat{q}_{\tau_y}(\tilde{p}) = \mathbf{B}^T(\tilde{p})\hat{\beta}_{\tau_y}, \quad \text{where} \quad (\text{C.2})$$

where

$$\hat{\beta}_{\tau_p} = \min_{\beta} \sum_{t=1}^T \rho_{\tau_p}(\tilde{p}_t - \beta), \quad \text{and} \quad (\text{C.3})$$

$$\hat{\beta}_{\tau_y} = \min_{\beta} \sum_{t=1}^T \sum_{j=1}^{n_t} \rho_{\tau_y}(\tilde{y}_{jt} - \mathbf{B}(\tilde{p}_t)\beta) + \frac{\lambda}{2} \beta^T \mathbf{D}_2^T \mathbf{D}_2 \beta. \quad (\text{C.4})$$

Again, λ is chosen via generalized approximate cross validation (Yuan (2006)); while we can include the penalty term in (C.3), no function that needs to be smoothed, and the value of the smoothing parameter λ does not impact the value of our estimate $\hat{\beta}_{\tau_p}$.

By the inverse probability transformation, $\{\tilde{p}_r^* = \hat{q}_{\tau_p,r}, \tilde{y}_r^* = \hat{q}_{\tau_y,r}(\tilde{p}_r^*)\}_{r=1}^R$ are R independent samples from $g(\tilde{y}, \tilde{p})$ where $\{\tau_{p,r}\}_{r=1}^R$ and $\{\tau_{y,r}\}_{r=1}^R$ are *Uniform*(0, 1) random variables, and using the methodology outlined in Section B of the online supplement, $\{y_{2020,r}^*, p_{2020,r}^*\}_{r=1}^R$ become R independent samples from $g(y_{2020}, p_{2020})$.

D Additional Simulation Study

In this section, we present the simulation study as first outlined in Section 4 of the main text where we assume a linear mean and standard deviation for the harvest price. Specifically, we assume

- $\mu_{\tilde{p}}(\tilde{s}) = 0.2 - 0.4\tilde{s}, \sigma_{\tilde{p}}(\tilde{s}) = 0.5 - 0.5\tilde{s}_t,$
- $\mu_{\tilde{y}}(\tilde{p}, \tilde{s}) = -25 + 14.45 \exp\{\tilde{p}_t\} + 22.18\tilde{s}_t,$ and $\sigma_{\tilde{y}} = 33$

Once again, we assume $\tilde{s}_t \stackrel{iid}{\sim} \text{Beta}(7, 44).$

Figure A-1 presents the true versus estimated τ_p^{th} -quantile functions for $\tau_p \in \{0.1, 0.25, 0.5, 0.75, 0.9\}$ for non-linear \tilde{p} . For each plot, the solid black line represents the true quantile function, the solid red line represents the median of the M estimated quantile functions, and the dashed red lines represent the 0.025 and 0.975 quantiles of the M estimated quantile functions. Based on the outcome of these graphs, the true quantile functions appears to directly overlap the median of the M estimated quantile functions, and the 0.025 and 0.975 quantile function bands fall close to the true quantile functions, suggesting our method does a good job of approximating the quantile functions of detrended prices \tilde{p} .

We also present the true versus estimated τ_y^{th} - quantile functions for \tilde{y} with $\tau_y \in \{0.1, 0.25, 0.5, 0.75, 0.9\}$ and $\tilde{s} \in \{0.08, 0.103, 0.133, 0.167, 0.201\}$, which are the 0.1, 0.25, 0.5, 0.75, and 0.9 quantiles of the Beta distribution used to simulate \tilde{s}_t . Figure A-2 plots the quantiles for \tilde{y} with non-linear \tilde{p} . Again, the true quantile functions are almost identical with the median of the M estimated quantile functions, and the 0.025 and 0.975 quantile function bands fall very close to the true quantile functions, indicating our method can estimate the quantile functions of detrended yields \tilde{y} well.

Figure A-3 illustrates the comparisons of the true and approximate kernel density plots of $g(\tilde{y}, \tilde{p}|\tilde{s})$ for $\tilde{s} = 0.103, 0.133, 0.1767$, demonstrating that the estimated density obtained from our draws closely aligns with the true joint densities, even when viewed from different angles. We further perform a 2-dimensional Kolmogorov-Smirnov test, as proposed in Fasano & Franceschini (1987), on all 100 Monte Carlo samples to assess the agreement between these two bivariate densities. The average p-values across the 100 samples are 0.41, 0.64, and 0.81 for $\tilde{s} = 0.103, 0.133, 0.1767$ respectively. These relatively large p-values, combined with the visual comparisons in Figure A-3, indicate that our SQR-based sampling method effectively generates valid samples from the target joint price and yield density.

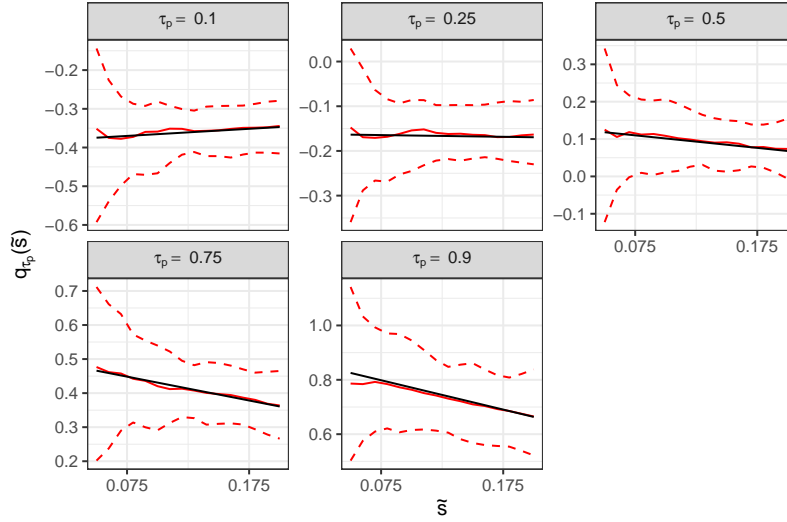


Figure A-1: True and estimated quantile functions of \tilde{p} from the linear \tilde{p} simulation study. Presented are the medians (solid red lines) and 0.025 and 0.975 quantiles (dashed red lines) of the MC estimates for the quantile regression function $q_{\tau_p}(\tilde{s}_t)$ against the associated “true” quantile curve (solid black lines). Each plot represents a different $\tau_p \in \{0.1, 0.25, 0.5, 0.75, 0.9\}$.

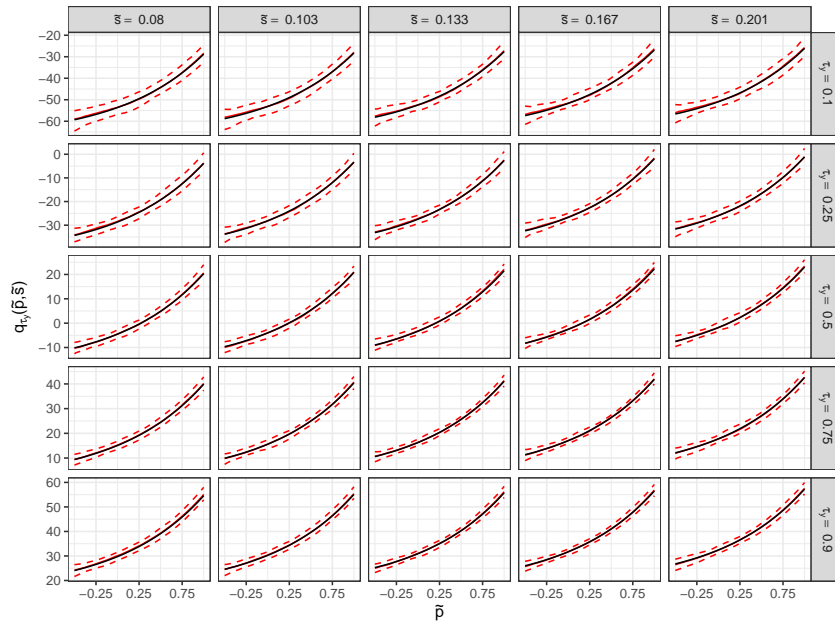


Figure A-2: True and estimated quantile functions of \tilde{y} from the linear \tilde{p} and non-linear \tilde{y} simulation study. Presented are the medians (solid red lines) and 0.025 and 0.975 quantiles (dashed red lines) of the MC estimates for the quantile regression function $q_{\tau_y}(\tilde{p}_t, \tilde{s}_t)$ against the associated “true” quantile curve (solid black lines). Each row represents a different $\tau_y \in \{0.1, 0.25, 0.5, 0.75, 0.9\}$ and each column represents the $\{0.1, 0.25, 0.5, 0.75, 0.9\}$ quantiles of the distribution of \tilde{s} .

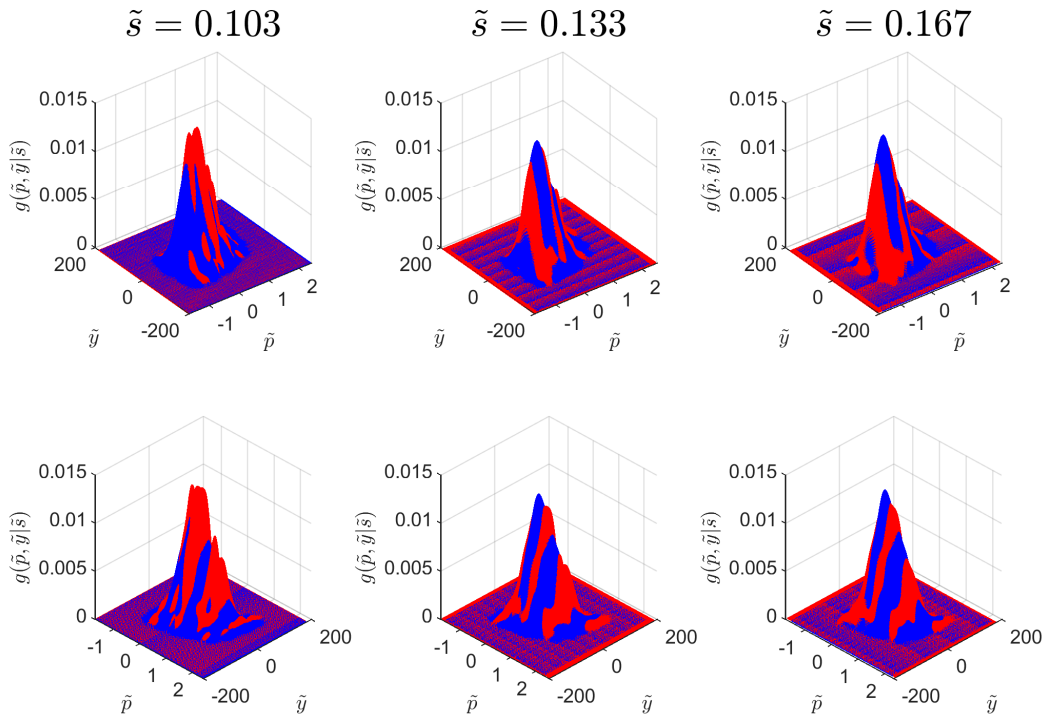


Figure A-3: 3d kernel density plots for the approximate joint density ($\hat{g}(\tilde{y}, \tilde{p}|\tilde{s})$) in red and the true joint density ($g(\tilde{y}, \tilde{p}|\tilde{s})$) in blue for the linear \tilde{p} and non-linear \tilde{y} simulation study. Each column represents a different value of $\tilde{s} \in \{0.103, 0.133, 0.167\}$ and each row represents a different viewing angle of the plot.

E Empirical Soybean Results

This section provides the empirical results for the soybean crop dataset, using the same timeline in the corn crop dataset in section 5 of the main text. Note, the conclusions of the soybean results are similar to those of the corn results.

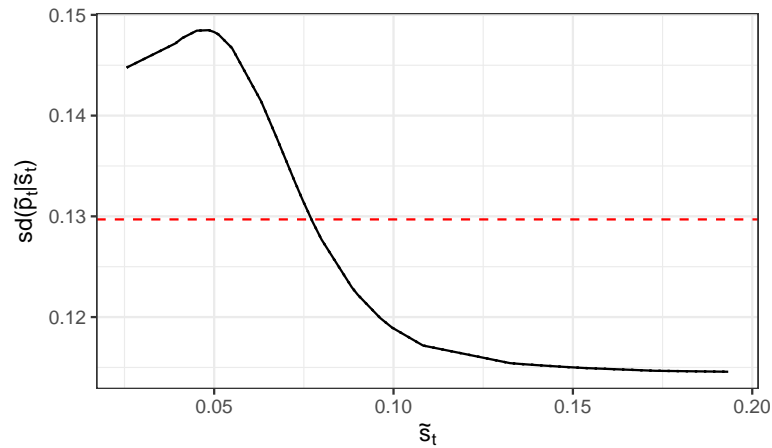


Figure A-4: Standard deviation of harvest price for soybean crops from 1990-2018 (in 2020 units). The dashed red line is the estimate of the unconditional standard deviation and the solid black line is the estimate of the conditional standard deviation function.

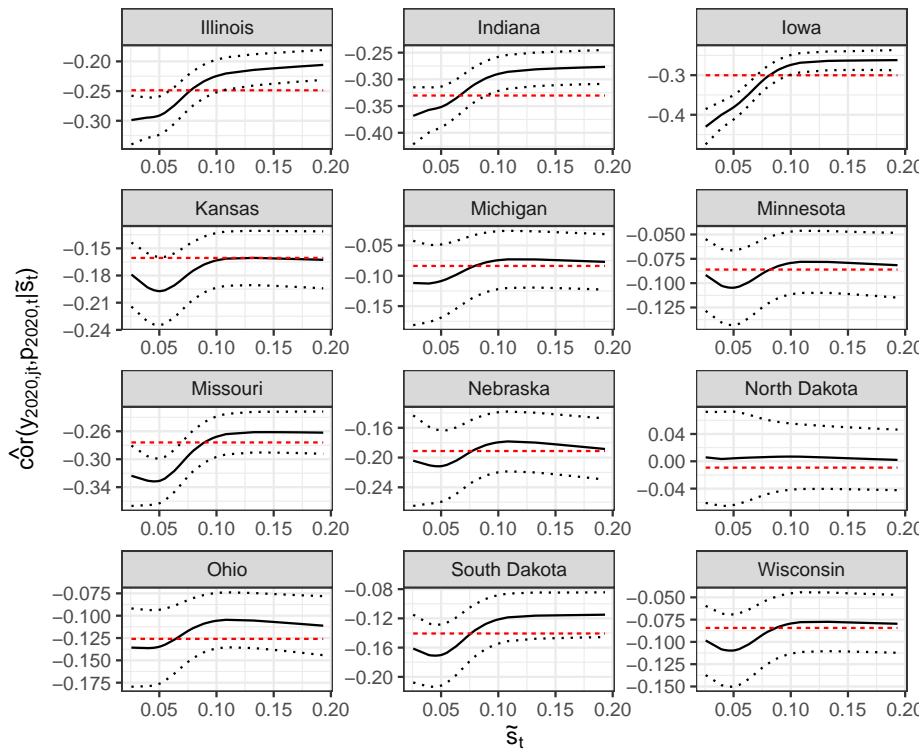


Figure A-5: Correlation of harvest price and county-level yield for soybean crops by state from 1990-2018 (in 2020 units). The dashed red line is the estimate of the unconditional correlation, the solid black line is the estimate of the conditional correlation function, and the dotted black lines are the 95% confidence bands for the conditional correlation function.

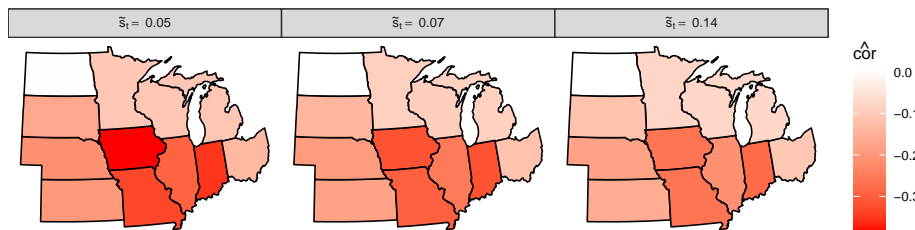


Figure A-6: Heat map of the conditional correlation of harvest price and county-level yield for soybean crops across states for the observed 0.2- (left panel), 0.5- (middle panel), and 0.8- (right panel) quantiles of leftover stocks. Darker shades of red represent states with more negative correlation.

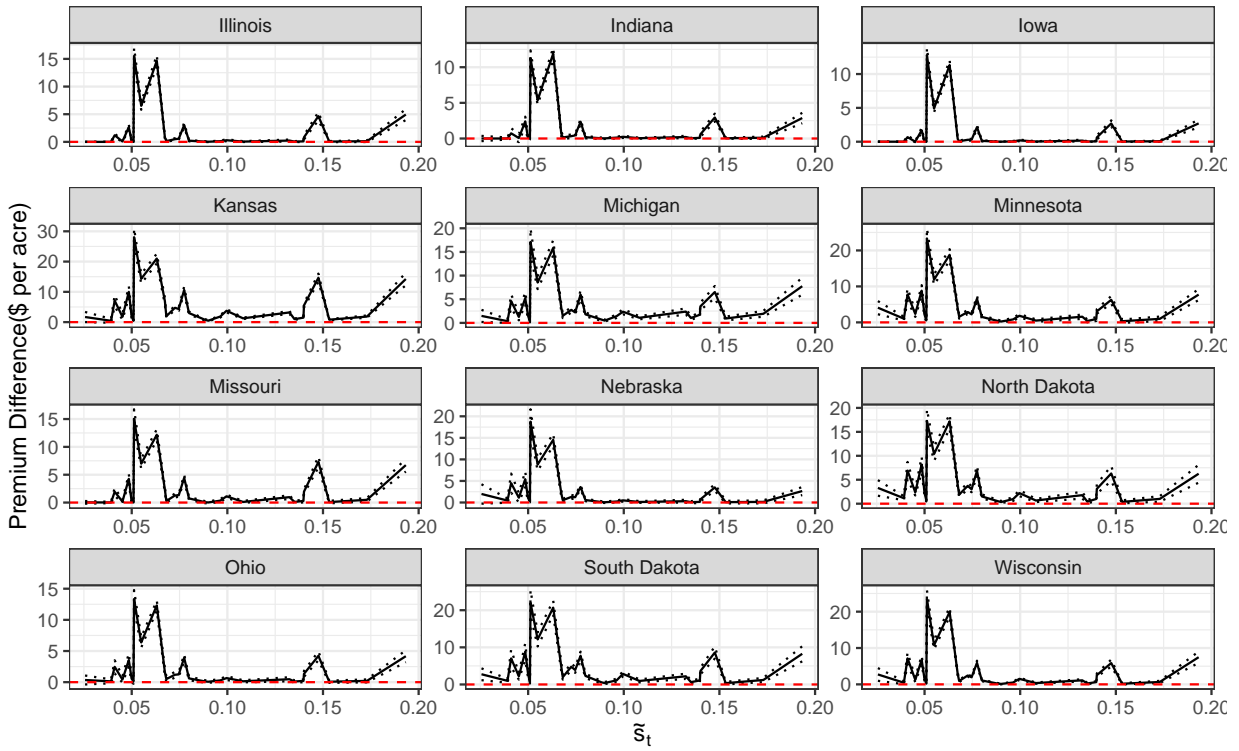


Figure A-7: Estimated difference in the proposed insurance premium and the imputed current insurance premium ($\psi = 0.7$) for soybean crops by state from 1990-2018 (in 2020 units). The dashed red line is a reference line at 0, and the gray shaded area is a reference for when spring future's price increased significantly.